



HAL
open science

MOTION EQUATIONS IN A KERR-NEWMAN-DE SITTER SPACE-TIME: SOME METHODS OF INTEGRATION AND APPLICATION TO BLACK HOLES SHADOWING IN SCILAB

Arthur Garnier

► **To cite this version:**

Arthur Garnier. MOTION EQUATIONS IN A KERR-NEWMAN-DE SITTER SPACE-TIME: SOME METHODS OF INTEGRATION AND APPLICATION TO BLACK HOLES SHADOWING IN SCILAB. 2022. hal-03762454

HAL Id: hal-03762454

<https://hal.science/hal-03762454>

Preprint submitted on 27 Aug 2022

HAL is a multi-disciplinary open access archive for the deposit and dissemination of scientific research documents, whether they are published or not. The documents may come from teaching and research institutions in France or abroad, or from public or private research centers.

L'archive ouverte pluridisciplinaire **HAL**, est destinée au dépôt et à la diffusion de documents scientifiques de niveau recherche, publiés ou non, émanant des établissements d'enseignement et de recherche français ou étrangers, des laboratoires publics ou privés.

MOTION EQUATIONS IN A KERR–NEWMAN–DE SITTER SPACE-TIME: SOME METHODS OF INTEGRATION AND APPLICATION TO BLACK HOLES SHADOWING IN SCILAB

ARTHUR GARNIER

ABSTRACT. In this note, we recall some basic facts about the Kerr–Newman–(anti) de Sitter (KNdS) space-time and review several formulations and integration methods for the geodesic equation of a test particle in such a space-time. In particular, we introduce some basic general symplectic integrators in the Hamiltonian formalism and we re-derive the separated motion equations using Carter’s method.

After this theoretical background, we explain how to ray-trace a KNdS black hole, equipped with a thin accretion disk, using Scilab. We compare the accuracy and execution time of the previous methods, concluding that the Carter equations is the best one. Then, inspired by Hagihara, we make use of the Weierstrass elliptic functions to simplify the programs and give some illustrations, including a simulation of M87*.

CONTENTS

0. Introduction	2
1. The Kerr–Newman–(anti) de Sitter spacetime	3
1.1. Reminders on Einstein’s field equation and electromagnetic stress-energy tensor	3
1.2. The Kerr–Newman–(anti) de Sitter solution and its analytic extension	3
1.3. Kerr–Schild form and maximality of the extension	8
2. Several formulations and numerical schemes for the geodesic equation	9
2.1. Lagrangian and Hamiltonian formalisms	9
2.2. Symplectic schemes for Hamilton’s equations	10
3. Motion constants and Carter’s equations	12
3.1. Motion equations	12
3.2. Expressions for the motion constants	15
4. Polar formulation for RNdS trajectories and the Weierstrass elliptic function	16
4.1. Polar geodesic equation	17
4.2. Use of Weierstrass’ function \wp for photon orbits	17
5. Model for the accretion disk	19
5.1. Angular velocity of circular massive orbits	19
5.2. Blackbody radiation temperature and brightness	20
5.3. Gravitational redshift and Doppler effect	20
6. Implementation and comparison of the methods	21
6.1. Shadowing and the backward ray tracing method	21
6.2. Optimization of the shadowing process with \wp	24
6.3. Comparison of the accuracy and execution time of the integrators	24
6.4. Some illustrations and a simulation of M87*	27
Appendix A. Proof that the KNdS metric solves the Einstein-Maxwell equations	33
References	36

Date: August 27, 2022.

2020 Mathematics Subject Classification. Primary 83C57, 83C10, 83-10; Secondary 85A25, 83F05, 85-10.

0. INTRODUCTION

The aim of this work is double. First, we compare several formulations and integration methods for the geodesic equations associated to the general Kerr–Newman–(anti) de Sitter (KNdS) metric. Second, we exhibit some simple methods for shadowing a KNdS black hole in `Scilab 6.1.1`¹. These methods include a model for a thin accretion disk orbiting the black hole. This paper doesn't claim to present some new results in the area, but rather to give a self-contained mathematical introduction to it, with an emphasis on the numerical aspects. The Scilab scripts are available at https://github.com/arthur-garnier/knds_orbits_and_shadows.git.

After some reminders on Einstein's general theory of relativity, we introduce the KNdS metric as in [GH77] and re-prove that it maximally extends to an analytic metric satisfying the Maxwell-Einstein field equation, see Theorem 1.2.1.

Section 2 focuses on the geodesic equation of a (possibly charged) test particle in the KNdS space-time. It also considers some of the formulations that can be used to numerically solve it, such as the Lagrangian and Hamiltonian formalisms. The latter is nice since it has some nice symplectic geometric properties. We then remind some classical general symplectic schemes which we implement. As we will later integrate the geometric equation *backwards*, the symplectic schemes that are *reversible* are of particular interest. However, we shall see that they will all present some instabilities around the symmetry axis and moreover, these methods can be quite long to process as the stable ones are implicit. To get rid of this issue, we use the method from [Car68].

Carter's method consists in identifying a fourth motion constant that make the geodesic equation *integrable*. This is done in Section 3. The resulting differential system is much simpler than the original one and can be solved quite easily using the routine `lode` for `Scilab 6.1.1` (see [Hin80]). For more details, see Theorem 3.1.1 and Corollary 3.1.2. In Proposition 3.2.1, we derive the motion constants from the *rest mass* and the initial data of the geodesic.

In the next Section 4, we treat the particular case of a non-rotating black hole. Following the original idea of [Hag30], we consider planar geodesics, parametrized in polar coordinates. In the case of a photon orbit in the *Reissner–Nordström–(anti) de Sitter black hole* (i.e. a non-rotating KNdS black hole), the geodesic equation can be reduced to the Weierstrass equation $\dot{\varphi}^2 = 4\varphi^3 - g_2\varphi - g_3$, whose solution is a *Weierstrass elliptic function*; see Proposition 4.2.1. Coupled with the Carlson algorithm for elliptic integrals ([Car95]), this provides a very efficient and fast way to shadow an RNdS black hole, which we also implement, see Corollary 4.2.3.

Then, we explain how we choose our model for the thin accretion disk, based on [SS73] and [Spr95]. We assume that the matter in the accretion disk radiates as a blackbody and we use (a rescaled version of) Planck's law for the brightness. We also include the gravitational and Doppler redshift effects to the implementation. See Section 5 for more details.

In Section 6, we make some remarks on the implementation process and provide details about the *backward ray tracing* algorithm we use. We compare the different integration methods introduced earlier, in terms of motion constants conservation and execution times. Among others, we explain how the Weierstrass functions can be used to make the general shadowing program faster to execute. The Carter equations are by far the best integration method. We finish by giving some illustrations and a simulation of the M87 black hole.

¹Equipped with the IPCV package at <https://ipcv.scilab-academy.com/>.

1. THE KERR–NEWMAN–(ANTI) DE SITTER SPACETIME

1.1. Reminders on Einstein’s field equation and electromagnetic stress-energy tensor. In full generality, consider a Lorentzian 4-manifold $(\mathcal{M}, \mathbf{g})$ and let \mathbf{R} be its Ricci tensor. Let $R := \text{tr}_{\mathbf{g}}(\mathbf{R})$ be the Ricci (scalar) curvature and $\mathbf{G} := \mathbf{R} - \frac{1}{2}R\mathbf{g}$ be the associated *Einstein tensor*. Then, the *Einstein field equation (EFE)* is the following equality

$$(1) \quad \mathbf{G} + \Lambda \mathbf{g} = \kappa \mathbf{T},$$

where \mathbf{T} is a symmetric 2-tensor on \mathcal{M} , $\kappa := 8\pi G/c^4$ is the *Einstein gravitational constant* and $\Lambda \in \mathbb{R}$ is called the *cosmological constant*. In this case, notice that the Bianchi identity implies that the covariant derivative of \mathbf{T} vanishes. If $(x^\mu)_{\mu=0,1,2,3}$ is a (local) coordinate frame on \mathcal{M} , then the (EFE) can be (locally) rewritten as

$$(2) \quad R_{\mu\nu} - \frac{1}{2}Rg_{\mu\nu} + \Lambda g_{\mu\nu} = \frac{8\pi G}{c^4}T_{\mu\nu},$$

with $R = g^{\mu\nu}R_{\mu\nu}$ (using Einstein’s summation convention), the matrix $(g^{\mu\nu})_{\mu,\nu}$ being the inverse of the Gram matrix $\text{Mat}_{x^\mu}(\mathbf{g}) = (g(\partial_{x^\mu}, \partial_{x^\nu})) =: (g_{\mu\nu})$. To simplify the notation, we also denote partial derivatives (resp. covariant derivatives) using a comma (resp. a semicolon) low index. **In the following, we choose the signature $(-, +, +, +)$ for Lorentzian metrics and we use natural (Stoney) units where $G = c = 4\pi\epsilon_0 = 1$.** Notice that this implies that $\mu_0 = 4\pi$.

Recall that given a metric $\mathbf{g} = (g_{\mu\nu})$, a divergence-free contravariant vector $\mathbf{J} = (J^\mu)$ (i.e. such that $J^\mu{}_{;\mu} := \nabla_\mu J^\mu = 0$) and a totally antisymmetric 2-tensor $\mathbf{F} = (F_{\mu\nu})$, seen as a differentiable 2-form $\mathbf{F} = \frac{1}{2}F_{\mu\nu}dx^\mu \wedge dx^\nu$, we say that \mathbf{F} satisfies the *covariant Maxwell equations* if

$$(ME) \quad d\mathbf{F} = 0 = d^*\mathbf{F} + \mu_0^*\mathbf{J},$$

where $*(-)$ denotes the Hodge dual. In this case the vector J^μ is called the *current 1-form* and \mathbf{F} is the *electromagnetic field tensor*. We can translate these equations in coordinates:

$$\begin{cases} F_{\mu\nu,\lambda} + F_{\nu\lambda,\mu} + F_{\lambda\mu,\nu} = 0, \\ F^{\mu\nu}{}_{;\mu} = -4\pi J^\nu. \end{cases}$$

Moreover, on a contractible open subset of \mathcal{M} , the Poincaré lemma ensures the existence of a 1-form $\mathbf{A} = A_\mu dx^\mu$, called the *electromagnetic vector potential*, such that $\mathbf{F} = d\mathbf{A}$. In coordinates, this reads

$$F_{\mu\nu} = A_{\nu,\mu} - A_{\mu,\nu} = A_{\nu;\mu} - A_{\mu;\nu}.$$

Finally, the *electromagnetic stress-energy tensor* \mathbf{T} associated to the field \mathbf{F} is given in local coordinates by²

$$T_{\mu\nu} = \frac{1}{\mu_0} \left(g^{\alpha\beta} F_{\alpha\mu} F_{\beta\nu} - \frac{1}{4} g_{\mu\nu} F_{\alpha\beta} F^{\alpha\beta} \right).$$

Then, the resulting EFE is called the *Einstein-Maxwell equation (EME)* associated to $(\mathbf{g}, \mathbf{J}, \mathbf{F})$. In the case where $\mathbf{J} = 0$, we call it the *electro-vacuum Einstein-Maxwell equation*.

1.2. The Kerr–Newman–(anti) de Sitter solution and its analytic extension. We now recall what the Kerr–Newman–de Sitter metric is. For more details, see [HS17, §1.1], [KK09, §5, 6] or [GH77, §II]. Consider the manifold $\mathcal{M} := \mathbb{R}^2 \times \mathbb{S}^2$, equipped with *Boyer-Lindquist coordinates* (t, r, θ, ϕ) , where $(\theta, \phi) \in [0, \pi] \times [0, 2\pi[$ describe spherical coordinates on \mathbb{S}^2 . Fix four constants $\Lambda, M, Q, J \in \mathbb{R} \times \mathbb{R}_+^3$ and define $a := J/M$ if $M \neq 0$ and $a := J$ otherwise. Let $\lambda := \Lambda/3$ and $\chi := 1 + \lambda a^2$ and consider the following globally defined functions

$$\Sigma := r^2 + a^2 \cos^2 \theta, \quad \Delta_r := (1 - \lambda r^2)(r^2 + a^2) - 2Mr + Q^2, \quad \Delta_\theta := 1 + \lambda a^2 \cos^2 \theta.$$

²to be precise, this expression is valid only once a gauge where $A_\sigma J^\sigma = 0$ has been chosen, but we don’t need to be that subtle as we are interested only in vacuum solutions.

The *Kerr–Newman–(anti)de Sitter (KNdS) metric* is the metric defined on the open subset $\{\cos\theta(1 - \cos\phi)\Sigma\Delta_r\Delta_\theta \neq 0\}$ by the line element

$$(\text{KNdS}) \quad ds^2 = -\frac{\Delta_r}{\chi^2\Sigma}(dt - a\sin^2\theta d\phi)^2 + \frac{\Delta_\theta \sin^2\theta}{\chi^2\Sigma}(adt - (r^2 + a^2)d\phi)^2 + \Sigma\left(\frac{dr^2}{\Delta_r} + \frac{d\theta^2}{\Delta_\theta}\right).$$

It may be convenient to have the metric written in terms of matrices. Ordering the coordinates as (t, r, θ, ϕ) , we have

$$\mathbf{g} = \begin{pmatrix} \frac{a^2 \sin^2 \theta \Delta_\theta - \Delta_r}{\chi^2 \Sigma} & 0 & 0 & \frac{a \sin^2 \theta (\Delta_r - (r^2 + a^2) \Delta_\theta)}{\chi^2 \Sigma} \\ 0 & \frac{\Sigma}{\Delta_r} & 0 & 0 \\ 0 & 0 & \frac{\Sigma}{\Delta_\theta} & 0 \\ \frac{a \sin^2 \theta (\Delta_r - (r^2 + a^2) \Delta_\theta)}{\chi^2 \Sigma} & 0 & 0 & \frac{\sin^2 \theta ((r^2 + a^2)^2 \Delta_\theta - a^2 \sin^2 \theta \Delta_r)}{\chi^2 \Sigma} \end{pmatrix}$$

and

$$\mathbf{g}^{-1} = \begin{pmatrix} \frac{\chi^2 (a^2 \sin^2 \theta \Delta_r - (r^2 + a^2)^2 \Delta_\theta)}{\Sigma \Delta_r \Delta_\theta} & 0 & 0 & \frac{a \chi^2 (\Delta_r - (r^2 + a^2) \Delta_\theta)}{\Sigma \Delta_r \Delta_\theta} \\ 0 & \frac{\Delta_r}{\Sigma} & 0 & 0 \\ 0 & 0 & \frac{\Delta_\theta}{\Sigma} & 0 \\ \frac{a \chi^2 (\Delta_r - (r^2 + a^2) \Delta_\theta)}{\Sigma \Delta_r \Delta_\theta} & 0 & 0 & \frac{\chi^2 (\Delta_r - a^2 \sin^2 \theta \Delta_\theta)}{\Sigma \Delta_r \Delta_\theta \sin^2 \theta} \end{pmatrix}.$$

The following result is well-known (see for instance [KK09, §6] or [BL67]) and is recalled here for completeness:

Theorem 1.2.1. *Assume that $\chi > 0$ and consider the electromagnetic vector potential $\mathbf{A} = A_\mu dx^\mu$ defined on the open submanifold $\mathcal{U} := \mathcal{M} \setminus \{\Sigma = 0\}$ by*

$$\mathbf{A} = \frac{Qr}{\chi\Sigma}(dt - a\sin^2\theta d\phi).$$

Then the metric (KNdS) extends to a smooth Lorentzian metric on \mathcal{U} and the electromagnetic field $\mathbf{F} := d\mathbf{A}$ verifies the associated vacuum Maxwell equations. Moreover, the KNdS metric solves the electro-vacuum Einstein-Maxwell equation on \mathcal{U} .

Proof. First, we express the metric in Kerr coordinates, using its *principal null geodesics*. More precisely, consider the trajectory of a photon in the plane $\theta \equiv \pi/2$ with total energy $E = 1$ and total (azimuthal) angular momentum $L = aE$. Using equations (12), we see that the corresponding four-velocity is given by

$$(\dot{t}, \dot{r}, \dot{\theta}, \dot{\phi}) = \left(\frac{\chi^2(r^2 + a^2)}{\Delta_r}, \pm\chi, 0, \frac{a\chi^2}{\Delta_r} \right).$$

By rescaling the affine parameter $\lambda \rightsquigarrow \lambda/\chi^2$, and choosing the ingoing geodesic with $\dot{r} < 0$, the velocity is given by

$$l^\mu = \left(\frac{r^2 + a^2}{\Delta_r}, \frac{-1}{\chi}, 0, \frac{a}{\Delta_r} \right).$$

Now, the coordinates u and $\bar{\phi}$ replacing t and ϕ respectively, should be chosen to be constant along this world line, that is, we want $du/dr = d\bar{\phi}/dr = 0$. Hence, we introduce

$$\begin{cases} u := t + T(r), \\ \bar{\phi} := \phi + \Phi(r), \end{cases}$$

where T and Φ are respectively given by

$$T(r) = \chi \int_0^r \frac{\varrho^2 + a^2}{\Delta_r(\varrho)} d\varrho, \quad \Phi(r) = a\chi \int_0^r \frac{d\varrho}{\Delta_r(\varrho)} - \frac{\pi}{2}.$$

The constant in the definition of Φ ensures that the Kerr-Schild variables approach oblate spheroidal coordinates as M and Λ go to zero and doesn't change the metric. The 1-forms

dt and $d\phi$ can be expressed as

$$dt = du - dT = du - \frac{\chi(r^2 + a^2)dr}{\Delta_r}, \quad d\phi = d\bar{\phi} - d\Phi = d\bar{\phi} - \frac{a\chi dr}{\Delta_r}.$$

Then, the metric in these new coordinates reads

$$\begin{aligned} ds^2 &= \frac{-\Delta_r}{\chi^2 \Sigma} \left(du - \frac{\chi(r^2 + a^2)dr}{\Delta_r} - a \sin^2 \theta \left(d\bar{\phi} - \frac{a\chi dr}{\Delta_r} \right) \right)^2 \\ &\quad + \frac{\Delta_\theta \sin^2 \theta}{\chi^2 \Sigma} \left(a \left(du - \frac{\chi(r^2 + a^2)dr}{\Delta_r} \right) - (r^2 + a^2) \left(d\bar{\phi} - \frac{a\chi dr}{\Delta_r} \right) \right)^2 + \Sigma \left(\frac{dr^2}{\Delta_r} + \frac{d\theta^2}{\Delta_\theta} \right) \\ &= \frac{a^2 \sin^2 \theta \Delta_\theta - \Delta_r}{\chi^2 \Sigma} du^2 + \frac{\sin^2 \theta}{\chi^2 \Sigma} [\Delta_\theta (r^2 + a^2)^2 - \Delta_r a^2 \sin^2 \theta] d\bar{\phi}^2 \\ &\quad + \frac{\Sigma d\theta^2}{\Delta_\theta} + \frac{2dudr}{\chi} + \frac{2a \sin^2 \theta}{\chi^2 \Sigma} (\Delta_r - \Delta_\theta (r^2 + a^2)) dud\bar{\phi} - \frac{2a \sin^2 \theta}{\chi} drd\bar{\phi}. \\ &= \frac{-1}{\chi^2 \Sigma} \left[a^2 \sin^4 \theta \Delta_r d\bar{\phi}^2 + (\Delta_r - a^2 \sin^2 \theta \Delta_\theta) du^2 - 2a \sin^2 \theta (\Delta_r - (r^2 + a^2) \Delta_\theta) dud\bar{\phi} \right] \\ &\quad + \frac{\Sigma d\theta^2}{\Delta_\theta} + \frac{2dudr}{\chi} - \frac{2a \sin^2 \theta}{\chi} drd\bar{\phi} \\ &= \frac{-1}{\chi^2 \Sigma} [\Delta_r (du - a \sin^2 \theta d\bar{\phi})^2 - \sin^2 \theta \Delta_\theta (adu - (r^2 + a^2) d\bar{\phi})^2] + \frac{\Sigma d\theta^2}{\Delta_\theta} + \frac{2dudr}{\chi} - \frac{2a \sin^2 \theta}{\chi} drd\bar{\phi}. \end{aligned}$$

Defining $\bar{t} := u - r$, we obtain the KNdS metric in *Kerr coordinates* $(\bar{t}, r, \theta, \bar{\phi})$:

(3)

$$ds^2 = \frac{\Delta_\theta \sin^2 \theta [a d\bar{t} + adr - (r^2 + a^2) d\bar{\phi}]^2 - \Delta_r [d\bar{t} + dr - a \sin^2 \theta d\bar{\phi}]^2}{\chi^2 \Sigma} + \frac{\Sigma d\theta^2}{\Delta_\theta} + \frac{2dr}{\chi} [d\bar{t} + dr - a \sin^2 \theta d\bar{\phi}].$$

Since $\Lambda a^2 > -3$, we have $\Delta_\theta > 0$ and therefore the above metric is well-defined everywhere except for $\Sigma = 0$. However, computing the determinant of this metric, we find the same result as for Boyer-Lindquist coordinates, that is

$$\det(g_{\mu\nu}) = -\chi^{-4} \Sigma^2 \sin^2 \theta$$

and thus it is not clear yet that the metric is Lorentzian (non-degenerate) because $\det(g_{\mu\nu}) = 0$ for $\theta = 0, \pi$. Therefore, we still have to transform the metric and we shall use *Kerr-Schild coordinates* for this purpose.

Following [BL67, II, (2.6)] we define the following ‘‘Cartesian’’ Kerr-Schild coordinates

$$(4) \quad \begin{cases} x := \sqrt{r^2 + a^2} \sin(\theta) \cos(\bar{\phi} + \arctan(a/r)), \\ y := \sqrt{r^2 + a^2} \sin(\theta) \sin(\bar{\phi} + \arctan(a/r)), \\ z := r \cos(\theta). \end{cases}$$

The variable r becomes a function of (x, y, z) implicitly defined by the relation

$$\frac{x^2 + y^2}{r^2 + a^2} + \frac{z^2}{r^2} = 1.$$

We differentiate (4) and after some manipulations, we find the following relations

$$zdz = -r^2 \cos \theta \sin \theta d\theta + r \cos^2 \theta dr, \quad xdx + ydy + zdz = a^2 \cos \theta \sin \theta d\theta + r dr$$

as well as

$$xdy - ydx = (r^2 + a^2) \sin^2 \theta d\bar{\phi} - a \sin^2 \theta dr.$$

Thus, we find the expressions

$$\begin{cases} dr = \frac{r^2(xdx+ydy)+(r^2+a^2)zdz}{r\Sigma}, \\ d\theta = \frac{xdx+ydy+zdz-rdr}{a^2 \cos \theta \sin \theta} = \frac{\cos^2 \theta(xdx+ydy+zdz)-zdz}{\Sigma \cos \theta \sin \theta}, \\ d\bar{\phi} = \frac{a \sin^2 \theta dr + xdy - ydx}{(r^2+a^2) \sin^2 \theta}. \end{cases}$$

These yield

$$adr - (r^2 + a^2)d\bar{\phi} = \frac{ydx - xdy}{\sin^2 \theta}, \quad dr - a \sin^2 \theta d\bar{\phi} = \frac{r(xdx + ydy) + a(ydx - xdy)}{r^2 + a^2} + \frac{zdz}{r}$$

and we may now express the metric in these new variables as (we keep one “ dr ” for now in order to simplify the notation, but we’ll give the full expression below)

$$\begin{aligned} ds^2 = & \left[\frac{2dr}{\chi} - \frac{\Delta_r}{\chi^2 \Sigma} \left(d\bar{t} + \frac{r(xdx + ydy) + a(ydx - xdy)}{r^2 + a^2} + \frac{zdz}{r} \right) \right] \left(d\bar{t} + \frac{r(xdx + ydy) + a(ydx - xdy)}{r^2 + a^2} + \frac{zdz}{r} \right) \\ & + \frac{\Delta_\theta \sin^2 \theta}{\chi^2 \Sigma} \left(ad\bar{t} + \frac{ydx - xdy}{\sin^2 \theta} \right)^2 + \frac{(\cos^2 \theta(xdx + ydy + zdz) - zdz)^2}{\Sigma \Delta_\theta \cos^2 \theta \sin^2 \theta}. \end{aligned}$$

At this point we can formally³ compute the determinant of the metric and obtain

$$\det((g_{\mu\nu})_{\text{KS}}) = -\chi^{-4} \neq 0,$$

so that the metric is Lorentzian where it is defined. The first line above indeed is a smooth differential 2-form except on $\{\Sigma = 0\}$, so all we have to do is transform the second line. Consider the auxiliary spacial metric

$$d\sigma^2 := \frac{\Delta_\theta(ydx - xdy)^2}{\chi^2 \Sigma \sin^2 \theta} + \frac{(\cos^2 \theta(xdx + ydy + zdz) - zdz)^2}{\Sigma \Delta_\theta \cos^2 \theta \sin^2 \theta}.$$

Developing and factorizing this expression yields

$$\begin{aligned} d\sigma^2 = & \left(\frac{x^2 \cos^2 \theta}{\Delta_\theta} + \frac{y^2 \Delta_\theta}{\chi^2} \right) \frac{dx^2}{\Sigma \sin^2 \theta} + \left(\frac{y^2 \cos^2 \theta}{\Delta_\theta} + \frac{x^2 \Delta_\theta}{\chi^2} \right) \frac{dy^2}{\Sigma \sin^2 \theta} + \left(\frac{\cos^2 \theta}{\Delta_\theta} - \frac{\Delta_\theta}{\chi^2} \right) \frac{2xydx dy}{\Sigma \sin^2 \theta} \\ & + \frac{\sin^2 \theta z^2 dz^2}{\Sigma \Delta_\theta \cos^2 \theta} - \frac{2zdz}{\Sigma \Delta_\theta} (xdx + ydy). \end{aligned}$$

First, we transform the coefficient of dx^2 . Using (4), we have

$$\cos^2 \theta = \frac{z^2}{r^2}, \quad \sin^2 \theta = \frac{x^2 + y^2}{r^2 + a^2}, \quad \text{so that } \Delta_\theta = 1 + \lambda a^2 \cos^2 \theta = \frac{r^2 + \lambda a^2 z^2}{r^2}, \quad \Sigma = \frac{r^4 + a^2 z^2}{r^2},$$

and recalling that $\chi = 1 + \lambda a^2$, we compute

$$\begin{aligned} \frac{1}{\Sigma \sin^2 \theta} \left(\frac{x^2 \cos^2 \theta}{\Delta_\theta} + \frac{y^2 \Delta_\theta}{\chi^2} \right) &= \frac{x^2 \cos^2 \theta (1 + \lambda a^2)^2 + y^2 (1 + \lambda a^2 \cos^2 \theta)^2}{\chi^2 \Sigma \Delta_\theta \sin^2 \theta} \\ &= \frac{x^2 \cos^2 \theta + y^2 + \lambda^2 a^4 \cos^2 \theta (x^2 + y^2 \cos^2 \theta) + 2\lambda a^2 \cos^2 \theta (x^2 + y^2)}{\chi^2 \Sigma \Delta_\theta \sin^2 \theta} \\ &= \frac{(x^2 + y^2)(\Delta_\theta + \chi \lambda a^2 \cos^2 \theta) - \sin^2 \theta (x^2 + y^2 \lambda^2 a^4 \cos^2 \theta)}{\chi^2 \Sigma \Delta_\theta \sin^2 \theta} \\ &= \frac{(r^2 + a^2)(\Delta_\theta + \chi \lambda a^2 \cos^2 \theta) - x^2 - y^2 \lambda^2 a^4 \cos^2 \theta}{\chi^2 \Sigma \Delta_\theta} \\ &= \frac{(r^2 + a^2)(r^2 + \lambda a^2 z^2 + \chi \lambda a^2 z^2) - r^2 x^2 - y^2 \lambda^2 a^4 z^2}{\chi^2 r^2 \Sigma \Delta_\theta} \end{aligned}$$

³i.e. using only algebraic substitutions and simplifications

so that

$$\frac{1}{\Sigma \sin^2 \theta} \left(\frac{x^2 \cos^2 \theta}{\Delta_\theta} + \frac{y^2 \Delta_\theta}{\chi^2} \right) = r^2 \frac{(r^2 + a^2)(r^2 + \lambda a^2 z^2 (1 + \chi)) - r^2 x^2 - \lambda^2 a^4 y^2 z^2}{\chi^2 (r^4 + a^2 z^2)(r^2 + \lambda a^2 z^2)}.$$

Exchanging x and y gives a similar expression for the coefficient of dy^2 . Now we treat the $dx dy$ term. We have

$$\begin{aligned} \frac{2xy}{\Sigma \sin^2 \theta} \left(\frac{\cos^2 \theta}{\Delta_\theta} - \frac{\Delta_\theta}{\chi^2} \right) &= \frac{2xy [\chi^2 \cos^2 \theta - \Delta_\theta^2]}{\chi^2 \Sigma \Delta_\theta \sin^2 \theta} = \frac{2xy [\cos^2 \theta (1 + \lambda a^2)^2 - (1 + \lambda a^2 \cos^2 \theta)^2]}{\chi^2 \Sigma \Delta_\theta \sin^2 \theta} \\ &= \frac{2xy [\cos^2 \theta + \lambda^2 a^4 \cos^2 \theta - 1 - \lambda^2 a^4 \cos^4 \theta]}{\chi^2 \Sigma \Delta_\theta \sin^2 \theta} = \frac{2xy (\lambda^2 a^4 \cos^2 \theta - 1)}{\chi^2 \Sigma \Delta_\theta} \\ &= \frac{2xy r^2 (\lambda^2 a^4 z^2 - r^2)}{\chi^2 (r^4 + a^2 z^2)(r^2 + \lambda a^2 z^2)}. \end{aligned}$$

Finally, we compute the remaining terms:

$$\begin{aligned} \frac{\sin^2 \theta z^2 dz^2}{\Sigma \Delta_\theta \cos^2 \theta} - \frac{2z dz}{\Sigma \Delta_\theta} (x dx + y dy) &= \frac{r^2 (x^2 + y^2) dz^2}{(r^2 + a^2) \Sigma \Delta_\theta} - \frac{2z dz}{\Sigma \Delta_\theta} (x dx + y dy) \\ &= \frac{r^6 (x^2 + y^2) dz^2}{(r^2 + a^2)(r^4 + a^2 z^2)(r^2 + \lambda a^2 z^2)} - \frac{2z r^4 dz (x dx + y dy)}{(r^4 + a^2 z^2)(r^2 + \lambda a^2 z^2)} \\ &= \frac{r^4 dz [r^2 (x^2 + y^2) dz - 2z (r^2 + a^2) (x dx + y dy)]}{(r^2 + a^2)(r^4 + a^2 z^2)(r^2 + \lambda a^2 z^2)}. \end{aligned}$$

Gathering all, we obtain the full expression of the metric in Kerr-Schild coordinates:

$$\begin{aligned} ds^2 &= \left[\frac{2dr}{\chi} - \frac{\Delta_r}{\chi^2 \Sigma} \left(d\bar{t} + \frac{r(x dx + y dy) + a(y dx - x dy)}{r^2 + a^2} + \frac{z dz}{r} \right) \right] \left(d\bar{t} + \frac{r(x dx + y dy) + a(y dx - x dy)}{r^2 + a^2} + \frac{z dz}{r} \right) \\ &\quad + d\sigma^2 + \frac{a \Delta_\theta d\bar{t}}{\chi^2 \Sigma} (a \sin^2 \theta d\bar{t} + 2(y dx - x dy)), \end{aligned}$$

that is,

$$\begin{aligned} (5) \quad ds^2 &= \frac{2(r^2(x dx + y dy) + (r^2 + a^2)z dz)}{\chi(r^4 + a^2 z^2)} \left(r d\bar{t} + \frac{r^2(x dx + y dy) + ar(y dx - x dy)}{r^2 + a^2} + z dz \right) \\ &\quad - \frac{\Delta_r}{\chi^2 (r^4 + a^2 z^2)} \left(r d\bar{t} + \frac{r^2(x dx + y dy) + ar(y dx - x dy)}{r^2 + a^2} + z dz \right)^2 \\ &\quad + \frac{a(r^2 + \lambda a^2 z^2) d\bar{t}}{\chi^2 (r^4 + a^2 z^2)} \left(\frac{a(x^2 + y^2) d\bar{t}}{r^2 + a^2} + 2(y dx - x dy) \right) \\ &\quad + \frac{r^2}{(r^4 + a^2 z^2)(r^2 + \lambda a^2 z^2)} \left[\frac{(r^2 + a^2)(r^2 + \lambda a^2 z^2 (1 + \chi)) - r^2 x^2 - \lambda^2 a^4 y^2 z^2}{\chi^2} dx^2 \right. \\ &\quad \left. + \frac{(r^2 + a^2)(r^2 + \lambda a^2 z^2 (1 + \chi)) - r^2 y^2 - \lambda^2 a^4 x^2 z^2}{\chi^2} dy^2 + \frac{2xy(\lambda^2 a^4 z^2 - r^2)}{\chi^2} dx dy \right. \\ &\quad \left. + \frac{r^2 dz}{r^2 + a^2} (r^2 (x^2 + y^2) dz - 2z (r^2 + a^2) (x dx + y dy)) \right], \end{aligned}$$

where $r = r(x, y, z)$ is the positive solution⁴ of $\frac{x^2 + y^2}{r^2 + a^2} + \frac{z^2}{r^2} = 1$. It is now manifest that this metric is well-defined everywhere except on the ring $\{\Sigma = 0\} = \{z = 0, x^2 + y^2 = a^2\}$.

To prove that the potential $\mathbf{A} = Qr\chi^{-1}\Sigma^{-1}(dt - a \sin^2 \theta d\phi)$ solves the vacuum Maxwell equations and that the KNdS metric solves the associated EME, by smoothness of the metric

⁴explicitly: $r = \frac{1}{\sqrt{2}} \sqrt{x^2 + y^2 + z^2 - a^2 + \sqrt{a^2(a^2 - 2x^2 - 2y^2 + 2z^2) + (x^2 + y^2 + z^2)^2}}$

and the potential, it suffices to check them on the dense open chart $\{\sin\theta(1-\cos\phi)\Delta_r\Sigma \neq 0\}$ and this relies on tedious but elementary calculations. Details are given in Appendix A. \square

Remark 1.2.2. *By the Christodoulou-Ruffini mass formula (see [Pra14, §4, formula 57]), when $M \rightarrow 0$, the irreducible mass approaches $\sqrt{-Q^2}/2$ and then also $Q \rightarrow 0$. Using the notation of the previous proof, we have*

$$\begin{aligned} \lim_{M \rightarrow 0} \bar{\phi} &= \phi + \lim_{M \rightarrow 0} \int_0^r \frac{a\chi d\varrho}{\Delta_r(\varrho)} - \frac{\pi}{2} = \phi + \int_0^r \frac{a\chi d\varrho}{(1-\lambda\varrho^2)(\varrho^2+a^2)} - \frac{\pi}{2} \\ &= \phi + \sqrt{\lambda} \operatorname{argth}(r\sqrt{\lambda}) + \arctan\left(\frac{r}{a}\right) - \frac{\pi}{2}. \end{aligned}$$

Therefore, when $M \rightarrow 0$, the Kerr-Schild coordinates (4) read

$$\begin{cases} x = \sqrt{r^2 + a^2} \sin(\theta) \cos(\phi + \sqrt{\lambda} \operatorname{argth}(r\sqrt{\lambda})), \\ y = \sqrt{r^2 + a^2} \sin(\theta) \sin(\phi + \sqrt{\lambda} \operatorname{argth}(r\sqrt{\lambda})), \\ z = r \cos(\theta), \end{cases}$$

where it is understood that $\sqrt{\lambda} \operatorname{argth}(r\sqrt{\lambda}) = -\sqrt{|\lambda|} \arctan(r\sqrt{|\lambda|})$ for $\lambda < 0$. Regarding the time coordinate, we have

$$\lim_{M \rightarrow 0} \bar{t} = t - r + \lim_{M \rightarrow 0} \int_0^r \frac{\chi(\varrho^2 + a^2) d\varrho}{\Delta_r(\varrho)} = t - r + \frac{\chi}{\sqrt{\lambda}} \operatorname{argth}(r\sqrt{\lambda}),$$

with the same convention as before: $\operatorname{argth}(r\sqrt{\lambda})/\sqrt{\lambda} = \arctan(r\sqrt{|\lambda|})/\sqrt{|\lambda|}$ for $\lambda < 0$. Hence, with our convention, the Kerr-Schild coordinates coincide with the usual oblate spheroidal coordinates only for $\lambda \rightarrow 0$ and in this case, the Kerr-Schild and Boyer-Lindquist times agree.

1.3. Kerr–Schild form and maximality of the extension. The formula (3) above allows to write the KNdS metric in Kerr coordinates $(\bar{t}, r, \theta, \bar{\phi})$ as

$$ds^2 = ds_0^2 + \frac{2Mr - Q^2}{\chi^2 \Sigma} (d\bar{t} + dr - a \sin^2 \theta d\bar{\phi})^2,$$

where ds_0^2 is the KNdS metric with $M = Q = 0$. In Boyer-Lindquist coordinates, we have

$$ds_0^2 = -\frac{\widetilde{\Delta}_r}{\chi^2 \Sigma} (dt - a \sin^2 \theta d\phi)^2 + \frac{\Delta_\theta \sin^2 \theta}{\chi^2 \Sigma} (adt - (r^2 + a^2) d\phi)^2 + \Sigma \left(\frac{dr^2}{\widetilde{\Delta}_r} + \frac{d\theta^2}{\Delta_\theta} \right),$$

where $\widetilde{\Delta}_r = (1 - \lambda r^2)(r^2 + a^2)$. As indicated in [HV21, §4.2], if we define new coordinates (T, R, Θ, Φ) by

$$T := t/\chi, \quad R^2 := \frac{1}{\chi}(r^2 \Delta_\theta + a^2 \sin^2 \theta), \quad R \cos \Theta = r \cos \theta, \quad \Phi = \phi - \frac{a\lambda}{\chi} T,$$

then the metric ds_0^2 becomes

$$ds_0^2 = -(1 - \lambda R^2) dT^2 + \frac{dR^2}{1 - \lambda R^2} + R^2 (d\Theta^2 + \sin^2 \Theta d\Phi^2),$$

which is the usual de Sitter metric. Thus, we obtain the *Kerr-Schild form* of the KNdS metric: the flat de Sitter metric plus a perturbation term. In Kerr-Schild coordinates, we have

$$ds^2 = ds_0^2 + \frac{2Mr - Q^2}{r^4 + a^2 z^2} \left(\frac{rd\bar{t}}{\chi} + \frac{r^2(xdx + ydy) + ar(ydx - xdy)}{\chi(r^2 + a^2)} + \frac{zdz}{\chi} \right)^2.$$

On the other hand, the Kretschmann scalar $K = R_{\alpha\beta\gamma\delta}R^{\alpha\beta\gamma\delta}$ for the KNdS metric has recently been computed by Kraniotis [Kra22, Theorem 1] and is given by

$$K = \frac{8}{\Sigma^6} \left[3\lambda^2 a^{12} \cos^{12} \theta + 18\lambda^2 a^{10} r^2 \cos^{10} \theta + 45\lambda^2 a^8 r^4 \cos^8 \theta + 6 \cos^6 \theta (10\lambda^2 a^6 r^6 - a^6 M^2) \right. \\ \left. + a^4 \cos^4 \theta (45\lambda^2 r^8 + 90M^2 r^2 - 60MQ^2 r + 7Q^4) \right. \\ \left. + a^2 r^2 \cos^2 \theta (18\lambda^2 r^2 - 90M^2 r^2 + 120MQ^2 r - 34Q^4) + 3\lambda^2 r^{12} + 6M^2 r^6 - 12MQ^2 r^5 + 7Q^4 r^4 \right].$$

It is singular exactly on $\{\Sigma = 0\}$ and thus the analytic extension of the KNdS metric to $\mathcal{M} \setminus \{\Sigma = 0\}$ is maximal.

2. SEVERAL FORMULATIONS AND NUMERICAL SCHEMES FOR THE GEODESIC EQUATION

Here, we first recall two of the main formulations of the geodesic equation namely, the Euler–Lagrange and Hamilton equations. Then, we review some of the general elementary symplectic integrators that can be used.

Throughout this section, we consider a geodesic $\gamma = (t, r, \theta, \phi)$ in the KNdS spacetime, corresponding to the trajectory of a test particle with rest mass $\mu \in \{-1, 0\}$, electric charge e , energy E , angular momentum L and Carter constant κ . Recall that γ satisfies the *geodesic equation*

$$(6) \quad \ddot{\gamma}^\mu + \Gamma^\mu_{\alpha\beta} \dot{\gamma}^\alpha \dot{\gamma}^\beta = e F^\mu_{\alpha} \dot{\gamma}^\alpha,$$

where $\Gamma^\mu_{\alpha\beta} = g^{\mu\nu} \Gamma_{\mu\alpha\beta} := \frac{1}{2} g^{\mu\nu} (g_{\nu\beta,\alpha} + g_{\nu\alpha,\beta} - g_{\alpha\beta,\nu})$ are the Christoffel symbols and $F^\mu_{\alpha} = g^{\mu\nu} F_{\nu\alpha}$ is the electromagnetic tensor (in mixed form). We assume that γ is a maximal solution of this equation, defined on an open interval $I \subset \mathbb{R}$, say, with affine parameter $\ell \in I$ (the dot of course represents the derivative with respect to the affine parameter).

2.1. Lagrangian and Hamiltonian formalisms. Consider the relativistic *Lagrangian* $\mathcal{L} : T\mathcal{M} \rightarrow \mathbb{R}$, defined by

$$\mathcal{L}(\gamma, \dot{\gamma}) := \frac{1}{2} g_{\mu\nu} \dot{\gamma}^\mu \dot{\gamma}^\nu + e A_\mu \dot{\gamma}^\mu,$$

as well as the related *action integral*

$$S := \int \mathcal{L}(\gamma, \dot{\gamma}) d\ell,$$

where we integrate on a compact sub-interval of I . Hamilton’s principle asserts that γ is a stationary point of the action S , and this is equivalent to the *Euler–Lagrange equation*

$$(7) \quad \frac{d}{d\ell} \left(\frac{\partial \mathcal{L}}{\partial \dot{\gamma}} \right) = \frac{\partial \mathcal{L}}{\partial \gamma}.$$

Developing, we find that for all $\mu \in \{0, 1, 2, 3\}$,

$$g_{\mu\nu} \ddot{\gamma}^\nu + g_{\mu\alpha,\beta} \dot{\gamma}^\alpha \dot{\gamma}^\beta + e A_{\mu,\alpha} \dot{\gamma}^\alpha = \frac{d}{d\ell} (g_{\mu\alpha} \dot{\gamma}^\alpha + e A_\mu) = \frac{1}{2} g_{\alpha\beta,\mu} \dot{\gamma}^\alpha \dot{\gamma}^\beta + e A_{\alpha,\mu} \dot{\gamma}^\alpha$$

and rearranging this yields

$$g_{\mu\nu} \ddot{\gamma}^\nu + \frac{1}{2} (2g_{\mu\alpha,\beta} - g_{\alpha\beta,\mu}) \dot{\gamma}^\alpha \dot{\gamma}^\beta + e (A_{\mu,\alpha} - A_{\alpha,\mu}) \dot{\gamma}^\alpha = 0,$$

or, equivalently,

$$(8) \quad \ddot{\gamma}^\mu + {}' \Gamma^\mu_{\alpha\beta} \dot{\gamma}^\alpha \dot{\gamma}^\beta - e F^\mu_{\alpha} \dot{\gamma}^\alpha = 0,$$

where

$${}' \Gamma^\mu_{\alpha\beta} = g^{\mu\nu} (g_{\alpha\nu,\beta} - \frac{1}{2} g_{\alpha\beta,\nu}).$$

This is indeed equivalent to (6) since the difference ${}' \Gamma^\mu_{\alpha\beta} - \Gamma^\mu_{\alpha\beta} = \frac{1}{2} g^{\mu\nu} (g_{\nu\alpha,\beta} - g_{\nu\beta,\alpha})$ is anti-symmetric in the indices α and β . However, we implement⁵ the geodesic equation in Euler–Lagrange form, as it requires a bit less heavy calculations than the genuine Christoffel

⁵Except for the Carter equations, we only implemented the case where $e = 0$ to simplify.

symbols. To solve the equations (8), we simply use the internal solver from Scilab that implements Adams methods (see [Hin80]).

Instead of the Lagrangian, one may look at the *Hamiltonian*. First, we introduce the *conjugate momenta*:

$$p_\mu := g_{\mu\nu}\dot{\gamma}^\nu + eA_\mu.$$

The Hamiltonian $\mathcal{H} : T^*\mathcal{M} \rightarrow \mathbb{R}$ is then defined as the Legendre transform of \mathcal{L} , namely

$$\mathcal{H}(\gamma, p) := \frac{1}{2}g^{\mu\nu}(p_\mu - eA_\mu)(p_\nu - eA_\nu) = p_\mu\dot{\gamma}^\mu - \mathcal{L}(\gamma, \dot{\gamma}).$$

Then, the Euler–Lagrange equation is equivalent to *Hamilton’s equations*

$$(9) \quad \begin{cases} \frac{d\gamma}{d\ell} = \frac{\partial\mathcal{H}}{\partial p}, \\ \frac{dp}{d\ell} = -\frac{\partial\mathcal{H}}{\partial\gamma}. \end{cases}$$

Unravelling this, we obtain the following system of order 1

$$(10) \quad \begin{cases} \dot{\gamma}^\mu = g^{\mu\alpha}(p_\alpha - eA_\alpha), \\ \dot{p}_\mu = \frac{e}{2}g^{\alpha\beta}(A_{\alpha,\mu}(p_\alpha - eA_\alpha) + A_{\beta,\mu}(p_\beta - eA_\beta)) - \frac{1}{2}g^{\alpha\beta}{}_{,\mu}(p_\alpha - eA_\alpha)(p_\beta - eA_\beta). \end{cases}$$

In the case of a particle without charge ($e = 0$), this reduces to

$$\begin{cases} \dot{\gamma}^\mu = g^{\mu\alpha}p_\alpha, \\ \dot{p}_\mu = -\frac{1}{2}g^{\alpha\beta}{}_{,\mu}p_\alpha p_\beta. \end{cases}$$

As we shall see in the comparison section, the equations are a bit faster to integrate (with the Adams solver from [Hin80]) than the Euler–Lagrange ones. Moreover, they are more efficient in preserving the Hamiltonian.

2.2. Symplectic schemes for Hamilton’s equations. In view of integrating the system (10), we may use general algorithms that apply to any Hamiltonian $\mathcal{H} : T^*\mathcal{X} \rightarrow \mathbb{R}$, called *symplectic integrators*. A detailed exposition can be found in [FQ10] and [HLW03]. See also [SSC94].

First, we remind some basics of symplectic geometry (see [FQ10, §3.1]). If $q = (q^1, \dots, q^N)$ are local coordinates on an N -manifold \mathcal{X} and $p = (p_1, \dots, p_N)$ the associated coordinates on $T_p^*\mathcal{X}$, then (q, p) are local coordinates on $T^*\mathcal{X}$ and we may define a symplectic form on it:

$$\omega := dp \wedge dq = dp_i \wedge dq^i.$$

If $\mathcal{H} : T^*\mathcal{X} \rightarrow \mathbb{R}$ is a smooth function, then there exists a vector field $X_{\mathcal{H}} \in \Gamma(T(T^*\mathcal{X}))$ on $T^*\mathcal{X}$ such that $\omega(X_{\mathcal{H}}, -) = d\mathcal{H}$. Then, given $(q, p) \in T^*\mathcal{X}$, there is a unique maximal curve $\gamma_{q,p} :]-\varepsilon, \varepsilon[\rightarrow T^*\mathcal{X}$ such that

$$\begin{cases} \gamma_{q,p}(0) = (q, p), \\ \gamma'_{q,p} = X_{\mathcal{H}} \circ \gamma_{q,p}. \end{cases}$$

Then, the *Hamiltonian flow* Φ_s is defined as $\Phi_s(q, p) := \gamma_{q,p}(s)$, when this makes sense. Citing [FQ10, §3.2.1, Theorem 2.4], this flow is *symplectic*, meaning that the pull-back $\Phi_s^*\omega = \omega$. In other words, if $\Phi'_s(q, p)$ denotes the Jacobian $(\partial\Phi_s/\partial(q, p))$ of Φ_s , then we have

$${}^t\Phi'_s(q, p) \cdot J \cdot \Phi'_s(q, p) = J, \quad \text{where } J := \begin{pmatrix} 0 & I_n \\ -I_n & 0 \end{pmatrix}$$

Roughly, this means that Hamilton’s equations (9) (or rather the flow of \mathcal{H}) preserves the symplectic structure on $T^*\mathcal{X}$. As we would like to solve the system numerically, it would be nice to have schemes that also preserve this geometric structure.

Consider a smooth curve $\xi : s \mapsto \xi(s) = (q(s), p(s))$ satisfying Hamilton’s equations

$$(11) \quad \begin{cases} \dot{q} = \partial_p\mathcal{H}(q, p), \\ \dot{p} = -\partial_q\mathcal{H}(q, p). \end{cases}$$

A one-step numerical scheme with step $h \neq 0$ can be represented by its *numerical flow* $\Phi_h : (q_n, p_n) \mapsto (q_{n+1}, p_{n+1})$. As for the Hamiltonian, this flow reflects the geometric properties of the scheme.

Definition 2.2.1. Define the involution $\psi : (q, p) \mapsto (q, -p)$ on $T^*\mathcal{X}$ and consider a numerical scheme with flow $\Phi_h : (q_n, p_n) \rightarrow (q_{n+1}, p_{n+1})$.

(1) The Hamiltonian \mathcal{H} is said to be time-reversible if its flow Φ_s satisfies

$$\psi \circ \Phi_s \circ \psi = \Phi_{-s}.$$

In other words, this means that $(\widehat{q}, \widehat{p}) = \Phi_s(q, p)$ iff $\Phi_s(\widehat{q}, -\widehat{p}) = (q, -p)$.

(2) Similarly, if \mathcal{H} is time-reversible, then the scheme is reversible if its flow satisfies

$$\psi \circ \Phi_h \circ \psi = \Phi_{-h}.$$

(3) The scheme is symmetric if we have $\Phi_h^{-1} = \Phi_{-h}$.

(4) Finally, the scheme is symplectic if its flow is, i.e. if

$${}^t\Phi'_h(q, p) \cdot J \cdot \Phi'_h(q, p) = J.$$

Remark 2.2.2. To say that \mathcal{H} is reversible is equivalent to the following conditions

$$\partial_p \mathcal{H}(q, -p) = -\partial_p \mathcal{H}(q, p) \quad \text{and} \quad \partial_q \mathcal{H}(q, -p) = \partial_q \mathcal{H}(q, p).$$

From this we see that for instance, the Hamiltonian of an uncharged particle in the KNdS space-time is reversible.

We now give the symplectic schemes we have implemented. As is well-known, explicit schemes are unstable and the approximations they produce may blow-up, especially with problems like our geodesic one, where some (coordinate) singularities appear in the metric. However, the (velocity-)Verlet is a relatively good explicit alternative for our setting. With that being said, it turns out that all the schemes we present here do blow-up near the axis of rotation $\{\sin \theta = 0\} \subset \mathcal{M}$.

The simplest methods are the *semi-implicit Euler schemes*. These are given as follows:

Algorithm 1 q -implicit Euler scheme

Require: $h > 0, (q_0, p_0)$

- 1: **for** $n = 0, \dots$, **do**
 - 2: $q_{n+1} = q_n + h\partial_p \mathcal{H}(q_{n+1}, p_n)$
 - 3: $p_{n+1} = p_n - h\partial_q \mathcal{H}(q_{n+1}, p_n)$
 - 4: **end for**
-

Algorithm 2 p -implicit Euler scheme

Require: $h > 0, (q_0, p_0)$

- 1: **for** $n = 0, \dots$, **do**
 - 2: $p_{n+1} = p_n - h\partial_q \mathcal{H}(q_n, p_{n+1})$
 - 3: $q_{n+1} = q_n + h\partial_p \mathcal{H}(q_n, p_{n+1})$
 - 4: **end for**
-

As we shall see later, the p -implicit method is roughly twice as fast as the q -implicit one in our setting. This comes from the fact that our (uncharged) Hamiltonian $\mathcal{H} = \frac{1}{2}g^{\mu\nu}(q)p_\mu p_\nu$ is way easier to differentiate with respect to p (it is quadratic in p) than with respect to q and thus the equation $p_{n+1} = p_n - h\partial_q \mathcal{H}(q_n, p_{n+1})$ is more easily solved than the equation $q_{n+1} = q_n + h\partial_p \mathcal{H}(q_{n+1}, p_n)$.

A relatively strong explicit method is the *velocity Verlet* (or Verlet-leapfrog) scheme. As in [BRSS18, §3.3], the scheme with step size h is written as follows:

Algorithm 3 Velocity Verlet scheme

Require: $h > 0, (q_0, p_0)$

- 1: **for** $n = 0, \dots$, **do**
- 2: $p_{n+\frac{1}{2}} = p_n - \frac{h}{2} \partial_q \mathcal{H}(q_n, p_n)$
- 3: $q_{n+1} = q_n + h \partial_p \mathcal{H}\left(q_n, p_{n+\frac{1}{2}}\right)$
- 4: $p_{n+1} = p_{n+\frac{1}{2}} - \frac{h}{2} \partial_q \mathcal{H}(q_{n+1}, p_n)$
- 5: **end for**

Following [HLW03, §1.8, (1.25)], a more stable method is the *Störmer-Verlet scheme*, which reads (there’s a dual version of it, roughly by exchanging q and p and the signs accordingly)

Algorithm 4 Störmer-Verlet scheme

Require: $h > 0, (q_0, p_0)$

- 1: **for** $n = 0, \dots$, **do**
- 2: $q_{n+\frac{1}{2}} = q_n + \frac{h}{2} \partial_p \mathcal{H}\left(q_{n+\frac{1}{2}}, p_n\right)$
- 3: $p_{n+1} = p_n - \frac{h}{2} \left(\partial_q \mathcal{H}\left(q_{n+\frac{1}{2}}, p_n\right) + \partial_q \mathcal{H}\left(q_{n+\frac{1}{2}}, p_{n+1}\right) \right)$
- 4: $q_{n+1} = q_{n+\frac{1}{2}} + \frac{h}{2} \partial_p \mathcal{H}\left(q_{n+\frac{1}{2}}, p_{n+1}\right)$
- 5: **end for**

Because of its stability, this is the most efficient method, but it requires much more time to numerically solve the implicit equation for $q_{n+1/2}$.

We may summarize the properties of the above schemes in the following result:

Theorem 2.2.3 ([HLW03], [DGML09]). *The Euler schemes are of order 1 and symplectic but not symmetric (inverting the flow exchanges the two schemes) and not reversible (time-reversion takes each one to its explicit analogue).*

The Verlet scheme is symplectic, reversible, symmetric and of order 2.

Finally, the Störmer-Verlet scheme is symplectic, reversible, symmetric and of order 2 as well, but it is also stable.

3. MOTION CONSTANTS AND CARTER’S EQUATIONS

In this section, we take advantage of the form of the metric (in Boyer-Lindquist coordinates) and apply Carter’s method [Car68] to derive the motion equations in the KNdS space-time. More precisely, the Hamilton-Jacobi equation is separable and yields four constants of motion, making the geodesic equations separable. Then, we explain how to find the four constants from genuine initial conditions.

3.1. Motion equations. Consider the trajectory of charged particle, with electric charge $e \in \mathbb{R}$, and let γ be the corresponding (time-like or light-like) geodesic, defined on an open interval $0 \in I \subset \mathbb{R}$ with affine parameter $\ell \in I$ and assume γ has values in $\mathcal{M} \setminus \{\cos \theta(1 - \cos \phi)\Sigma \Delta_r = 0\}$. Recall the Hamiltonian

$$\frac{\mu}{2} := \mathcal{H}(\gamma, p) = \frac{1}{2} g^{\mu\nu} (p_\mu - eA_\mu)(p_\nu - eA_\nu)$$

which is constant along γ and equals $-\frac{1}{2}m^2$, where m is the rest mass of the particle⁶. Also, as ∂_t and ∂_ϕ are Killing vectors, the *total energy* $E := -p_t$ and the *total (azimuthal) angular*

⁶ $m = 0$ for a photon

momentum $L := p_\phi$ are constant along γ too. It turns out that there is a fourth constant κ , called the *Carter constant*, which allows to write the geodesic equations in a separable form. This is the point of the following well-known result (the formulation and proof are inspired by [BBS89], [HMS14] and [HS17]):

Theorem 3.1.1. *Given a geodesic γ as above, define the following functions on I :*

$$W_r := \chi(E(r^2 + a^2) - aL) + eQr \quad \text{and} \quad W_\theta := \chi(aE \sin \theta - L/\sin \theta).$$

Then, the quantity

$$\kappa := \Delta_\theta p_\theta^2 + \frac{W_\theta^2}{\Delta_\theta} - \mu a^2 \cos^2 \theta = -\Delta_r p_r^2 + \frac{W_r^2}{\Delta_r} + \mu r^2$$

is constant along γ and moreover, $\gamma = (t, r, \theta, \phi)$ satisfies the following differential system on I :

$$(12) \quad \begin{cases} \frac{\Sigma}{\chi} \dot{t} = \frac{W_r(r^2 + a^2)}{\Delta_r} - \frac{aW_\theta \sin \theta}{\Delta_\theta}, \\ \Sigma^2 \dot{r}^2 = W_r^2 - \Delta_r(\kappa - \mu r^2), \\ \Sigma^2 \dot{\theta}^2 = -W_\theta^2 + \Delta_\theta(\kappa + \mu a^2 \cos^2 \theta), \\ \frac{\Sigma}{\chi} \dot{\phi} = \frac{aW_r}{\Delta_r} - \frac{W_\theta}{\Delta_\theta \sin \theta}. \end{cases}$$

Proof. First, we compute the Hamiltonian explicitly:

$$\begin{aligned} 2\mathcal{H}(\gamma, p) &\stackrel{\text{df}}{=} g^{\mu\nu} (p_\mu - eA_\mu)(p_\nu - eA_\nu) = g^{tt} \left(p_t - \frac{eQr}{\chi\Sigma} \right)^2 + 2g^{t\phi} \left(p_t - \frac{eQr}{\chi\Sigma} \right) \left(p_\phi + \frac{eQra \sin^2 \theta}{\chi\Sigma} \right) \\ &\quad + g^{\phi\phi} \left(p_\phi + \frac{eQra \sin^2 \theta}{\chi\Sigma} \right)^2 + g^{rr} p_r^2 + g^{\theta\theta} p_\theta^2 \\ &= \frac{\chi^2}{\Sigma\Delta_r\Delta_\theta} (a^2 \sin^2 \theta \Delta_r - (r^2 + a^2)^2 \Delta_\theta) \left(E + \frac{eQr}{\chi\Sigma} \right)^2 + \frac{\chi^2}{\Sigma} \left(\frac{1}{\sin^2 \theta \Delta_\theta} - \frac{a^2}{\Delta_r} \right) \left(L + \frac{eQra \sin^2 \theta}{\chi\Sigma} \right)^2 \\ &\quad - \frac{2a\chi^2}{\Sigma\Delta_r\Delta_\theta} (\Delta_r - (r^2 + a^2)\Delta_\theta) \left(L + \frac{eQra \sin^2 \theta}{\chi\Sigma} \right) \left(E + \frac{eQr}{\chi\Sigma} \right) + \frac{\Delta_r}{\Sigma} p_r^2 + \frac{\Delta_\theta}{\Sigma} p_\theta^2. \end{aligned}$$

Formally developing and factorizing, we find

$$\begin{aligned} \mu &= \frac{1}{\Sigma^3 \Delta_r \Delta_\theta \sin^2 \theta} \left\{ -2\chi eQr \Sigma^2 \sin^2 \theta \Delta_\theta (E(r^2 + a^2) - aL) - r^2 e^2 Q^2 a^4 \sin^6 \theta \Delta_\theta \right. \\ &\quad \left. + a^2 \sin^4 \theta (2e^2 r^2 Q^2 (r^2 + a^2) \Delta_\theta + E^2 \chi^2 \Sigma^2 \Delta_r) + L^2 \chi^2 \Sigma^2 \Delta_r \right. \\ &\quad \left. + \sin^2 \theta [\Sigma^2 \Delta_\theta^2 \Delta_r p_\theta^2 + \Delta_\theta (\Sigma^2 (\Delta_r^2 p_r^2 - \chi^2 (E(r^2 + a^2) - aL)^2) - e^2 r^2 Q^2 (r^2 + a^2)^2) - 2ELa\chi^2 \Sigma^2 \Delta_r] \right\} \\ &= \frac{2\chi eQr}{\Sigma\Delta_r} (aL - E(r^2 + a^2)) - \frac{e^2 Q^2 r^2 a^4 \sin^4 \theta}{\Sigma^2 \Delta_r} + \frac{2a^2 e^2 Q^2 r^2 \sin^2 \theta (r^2 + a^2)}{\Sigma^2 \Delta_r} + \frac{a^2 \chi^2 E^2 \sin^2 \theta}{\Sigma\Delta_\theta} \\ &\quad + \frac{L^2 \chi^2}{\sin^2 \theta \Sigma\Delta_\theta} - \frac{2ELa\chi^2}{\Sigma\Delta_\theta} - \frac{\chi^2}{\Sigma\Delta_r} (E(r^2 + a^2) - aL)^2 - \frac{e^2 Q^2 r^2 (r^2 + a^2)^2}{\Sigma^2 \Delta_r} + \frac{\Delta_r}{\Sigma} p_r^2 + \frac{\Delta_\theta}{\Sigma} p_\theta^2 \\ &= \frac{e^2 Q^2 r^2}{\Sigma^3 \Delta_r} \underbrace{(2a^2 (r^2 + a^2) \sin^2 \theta - a^4 \sin^4 \theta - (r^2 + a^2)^2)}_{=-\Sigma^2} + \frac{L^2 \chi^2}{\Sigma\Delta_\theta \sin^2 \theta} + \frac{\Delta_r}{\Sigma} p_r^2 + \frac{\Delta_\theta}{\Sigma} p_\theta^2 \\ &\quad + \frac{aL - E(r^2 + a^2)}{\Sigma\Delta_r} (2\chi eQr + \chi^2 (E(r^2 + a^2) - aL)) + \frac{aE\chi^2}{\Sigma\Delta_\theta} (aE \sin^2 \theta - 2L) \end{aligned}$$

and so

$$\begin{aligned}
 \mu &= -\frac{e^2 Q^2 r^2}{\Sigma \Delta_r} + \frac{\chi(aL - E(r^2 + a^2))}{\Sigma \Delta_r} (2eQr + \chi(E(r^2 + a^2) - aL)) + \frac{a\chi^2 E}{\Sigma \Delta_\theta} (aE \sin^2 \theta - 2L) \\
 &\quad + \frac{L^2 \chi^2}{\Sigma \Delta_\theta \sin^2 \theta} + \frac{\Delta_r}{\Sigma} p_r^2 + \frac{\Delta_\theta}{\Sigma} p_\theta^2 \\
 &= -\frac{\chi^2}{\Sigma \Delta_r} \left(E(r^2 + a^2) - aL + \frac{eQr}{\chi} \right)^2 + \frac{\chi^2 (aE \sin^2 \theta - L)^2}{\Sigma \Delta_\theta \sin^2 \theta} + \frac{\Delta_r}{\Sigma} p_r^2 + \frac{\Delta_\theta}{\Sigma} p_\theta^2 \\
 &= \frac{1}{\Sigma} \left(-\frac{W_r^2}{\Delta_r} + \frac{W_\theta^2}{\Delta_\theta} + \Delta_r p_r^2 + \Delta_\theta p_\theta^2 \right).
 \end{aligned}$$

Therefore, the Hamiltonian is given by

$$(13) \quad \mathcal{H}(\gamma, p) = \frac{1}{2} \left(\frac{W_\theta^2}{\Sigma \Delta_\theta} - \frac{W_r^2}{\Sigma \Delta_r} + \frac{\Delta_r}{\Sigma} p_r^2 + \frac{\Delta_\theta}{\Sigma} p_\theta^2 \right).$$

Consider now the action integral

$$S := \int^\ell \mathcal{L}(\gamma, \dot{\gamma}) dl = \int^\ell p_\mu \dot{\gamma}^\mu - \mathcal{H}(\gamma, p) dl.$$

Then, we have $p_\mu = \partial S / \partial \dot{\gamma}^\mu$ and the motion equations can be expressed as the *Hamilton–Jacobi equation*

$$(14) \quad \frac{\partial S}{\partial \ell} = \mathcal{H} \left(\gamma, \frac{\partial S}{\partial \gamma} \right).$$

Using (13), this amounts to say that

$$\mu = 2 \frac{\partial S}{\partial \ell} = \frac{W_\theta^2}{\Sigma \Delta_\theta} - \frac{W_r^2}{\Sigma \Delta_r} + \frac{\Delta_r}{\Sigma} \left(\frac{\partial S}{\partial r} \right)^2 + \frac{\Delta_\theta}{\Sigma} \left(\frac{\partial S}{\partial \theta} \right)^2.$$

This equation may be rewritten in the separated form

$$\frac{W_\theta^2}{\Delta_\theta} + \Delta_\theta \left(\frac{\partial S}{\partial \theta} \right)^2 - \mu a^2 \cos^2 \theta = \frac{W_r^2}{\Delta_r} - \Delta_r \left(\frac{\partial S}{\partial r} \right)^2 + \mu r^2$$

so that each side of this equation is equal to some constant $\kappa \in \mathbb{R}$, as in the statement. But since we have $\Delta_\nu p_\nu = \Sigma \dot{\nu}$ for $\nu = r, \theta$, we obtain the equations for \dot{r}^2 and $\dot{\theta}^2$ as claimed.

Now, the equations for \dot{t} and $\dot{\phi}$ may be derived as follows. We compute

$$g^{t\mu} p_\mu = g^{t\mu} (g_{\mu\nu} \dot{\gamma}^\nu + eA_\mu) = \dot{t} + e g^{t\mu} A_\mu = \dot{t} + \frac{eQr}{\chi \Sigma} (g^{tt} - a \sin^2 \theta g^{t\phi}) = \dot{t} - \frac{\chi eQr(r^2 + a^2)}{\Sigma \Delta_r}$$

so that we get

$$\dot{t} = \frac{\chi eQr(r^2 + a^2)}{\Sigma \Delta_r} + g^{tt} p_t + g^{t\phi} p_\phi = \frac{\chi eQr(r^2 + a^2)}{\Sigma \Delta_r} - E g^{tt} + L g^{t\phi} = \frac{\chi W_r(r^2 + a^2)}{\Sigma \Delta_r} - \frac{a\chi W_\theta \sin \theta}{\Sigma \Delta_\theta}$$

and we proceed in the same way for $\dot{\phi}$: we have $g^{\phi\mu} p_\mu = \dot{\phi} - \frac{eQra\chi}{\Sigma \Delta_r}$ and thus

$$\dot{\phi} = \frac{eQra\chi}{\Sigma \Delta_r} + g^{t\phi} p_t + g^{\phi\phi} p_\phi = \frac{eQra\chi}{\Sigma \Delta_r} - E g^{t\phi} + L g^{\phi\phi} = \frac{a\chi W_r}{\Sigma \Delta_r} - \frac{\chi W_\theta}{\Sigma \Delta_\theta \sin \theta}.$$

□

The set of equations (12) unusable in numerical computations due to the squares in the equations for \dot{r} and $\dot{\theta}$. Indeed, at *turning points* (points where the sign of \dot{r} or $\dot{\theta}$ changes), one could not choose what sign to put in front of the square root when these get smaller and smaller. We get rid of this difficulty using the method of [FW04] (see also [PYYY16]) and derivate the equations for \dot{r}^2 and $\dot{\theta}^2$ again. It turns out the formulation is more elegant when dealing with the derivate conjugate momenta \dot{p}_r and \dot{p}_θ rather than with \dot{r} and $\dot{\theta}$.

Corollary 3.1.2. *With the same notation as in Theorem 3.1.1, the geodesic γ with motion constants (μ, E, L, κ) satisfies the following first order autonomous differential system with variables $(t, r, p_r, \theta, p_\theta, \phi)$:*

$$(15) \quad \left\{ \begin{array}{l} \frac{\Sigma \dot{t}}{\chi} = \frac{W_r(r^2 + a^2)}{\Delta_r} - \frac{aW_\theta \sin \theta}{\Delta_\theta}, \\ \Sigma \dot{r} = \Delta_r p_r, \\ \Sigma \dot{p}_r = \frac{\frac{\partial W_r^2}{\partial r} - \Delta'_r(\kappa - \mu r^2)}{2\Delta_r} + \mu r - \Delta'_r p_r^2, \\ \Sigma \dot{\theta} = \Delta_\theta p_\theta, \\ \Sigma \dot{p}_\theta = \frac{-\frac{\partial W_\theta^2}{\partial \theta} + \Delta'_\theta(\kappa + \mu a^2 \cos^2 \theta)}{2\Delta_\theta} - \mu a^2 \cos \theta \sin \theta - \Delta'_\theta p_\theta^2, \\ \frac{\Sigma \dot{\phi}}{\chi} = \frac{aW_r}{\Delta_r} - \frac{W_\theta}{\Delta_\theta \sin \theta}, \end{array} \right.$$

where, of course, for $\nu = r, \theta$, the symbol Δ'_ν means $\partial \Delta_\nu / \partial \nu$.

Proof. We only carry the calculations out for \dot{p}_r , the case of \dot{p}_θ being similar. Define $f(r) := \frac{W_r^2}{\Delta_r^2} - \frac{\kappa - \mu r^2}{\Delta_r}$ so that the second equation from (12) reads $p_r^2 = f(r)$ and differentiating this equation with respect to ℓ gives

$$\begin{aligned} 2p_r \dot{p}_r = \frac{\partial f}{\partial r} \frac{dr}{d\ell} &\iff \frac{2\Sigma \dot{p}_r}{\Delta_r} = \frac{\partial f}{\partial r} = 2 \frac{W_r(W'_r \Delta_r - W_r \Delta'_r)}{\Delta_r^3} - \frac{-2\mu r \Delta_r - (\kappa - \mu r^2) \Delta'_r}{\Delta_r^2} \\ &\iff \Sigma \dot{p}_r = \frac{W_r(W'_r \Delta_r - W_r \Delta'_r)}{\Delta_r^2} + \mu r + (\kappa - \mu r^2) \frac{\Delta'_r}{2\Delta_r} \\ &\iff \Sigma \dot{p}_r = \frac{2W'_r W_r - \Delta'_r(\kappa - \mu r^2)}{2\Delta_r} + \mu r + \frac{\Delta'_r}{\Delta_r} \left(\kappa - \mu r^2 - \frac{W_r^2}{\Delta_r} \right) \\ &\iff \Sigma \dot{p}_r = \frac{\partial_r(W_r^2) - \Delta'_r(\kappa - \mu r^2)}{2\Delta_r} + \mu r - \Delta'_r p_r^2. \end{aligned}$$

□

3.2. Expressions for the motion constants. In order to implement the set of equations (15), we need to find the constants (μ, E, L, κ) from initial values for the geodesic γ . We have the following result:

Proposition 3.2.1. *Given a geodesic $\gamma = (t, r, \theta, \phi)$ as in Theorem 3.1.1, the energy, angular momentum and Carter's constant are given as follows:*

$$\left\{ \begin{array}{l} E = -\frac{eQr}{\chi \Sigma} + \frac{1}{\chi} \sqrt{(a^2 \sin^2 \theta \Delta_\theta - \Delta_r) \left(\frac{\mu}{\Sigma} - \frac{\dot{r}^2}{\Delta_r} - \frac{\dot{\theta}^2}{\Delta_\theta} \right) + \frac{\dot{\phi}^2 \sin^2 \theta \Delta_r \Delta_\theta}{\chi^2}}, \\ L = \frac{\sin^2 \theta}{\chi^2 (\Delta_r - a^2 \sin^2 \theta \Delta_\theta)} \left[aE \chi^2 \Delta_r + \Delta_\theta \left(\Sigma \Delta_r \dot{\phi} - a \chi (\chi E (r^2 + a^2) + eQr) \right) \right], \\ \kappa = \frac{W_\theta^2 + \Sigma^2 \dot{\theta}^2}{\Delta_\theta} - \mu a^2 \cos^2 \theta = \frac{W_r^2 - \Sigma^2 \dot{r}^2}{\Delta_r} + \mu r^2, \end{array} \right.$$

where $\mu = -1$ for a massive test particle and $\mu = 0$ for a photon.

Proof. The expressions for κ are straightforwardly obtained from those in Theorem 3.1.1. To compute L , we simply invert the azimuthal equation from the system 12. We write

$$\frac{\Sigma \dot{\phi}}{\chi} = \frac{aW_r}{\Delta_r} - \frac{W_\theta}{\Delta_\theta \sin \theta} = \chi L \left(\frac{1}{\Delta_\theta \sin^2 \theta} - \frac{a^2}{\Delta_r} \right) - \frac{a\chi E}{\Delta_\theta} + \frac{a(\chi E(r^2 + a^2) + eQr)}{\Delta_r}$$

so that, multiplying both sides by $\sin^2 \theta \Delta_r \Delta_\theta$ yields

$$\begin{aligned} \chi L(\Delta_r - a^2 \sin^2 \theta \Delta_\theta) &= \frac{\Sigma \Delta_r \Delta_\theta \sin^2 \theta \dot{\phi}}{\chi} + a\chi E \Delta_r \sin^2 \theta - a \sin^2 \Delta_\theta (\chi E(r^2 + a^2) + eQr) \\ &= \frac{\sin^2 \theta}{\chi} \left[aE\chi^2 \Delta_r + \Delta_\theta \left(\Sigma \Delta_r \dot{\phi} - a\chi(\chi E(r^2 + a^2) + eQr) \right) \right] \end{aligned}$$

as claimed. Now for the energy, it is determined by $E \geq 0$ and the fact that $2\mathcal{H}(\gamma, p) \equiv \mu$. Recalling the equation (13) and using the above expression for L , we compute

$$2\mathcal{H} = \mu \iff \Sigma(\Delta_r - a^2 \sin^2 \theta \Delta_\theta)(\mu - 2\mathcal{H}) = 0 \iff \alpha_2 E^2 + \alpha_1 E + \alpha_0 = 0,$$

where

$$\alpha_2 = \chi^2 \Sigma^2, \quad \alpha_1 = 2\chi eQr \Sigma$$

and

$$\begin{aligned} \alpha_0 &= (\Delta_r - a^2 \sin^2 \theta \Delta_\theta) \left[\mu \Sigma - \frac{\Sigma^2 \dot{r}^2}{\Delta_r} - \frac{\Sigma^2 \dot{\theta}^2}{\Delta_\theta} + \frac{\left(eQr - \frac{a \sin^2 \theta \Delta_\theta (\Sigma \Delta_r \dot{\phi} - a\chi eQr)}{\chi(\Delta_r - a^2 \sin^2 \theta \Delta_\theta)} \right)^2}{\Delta_r} - \frac{\sin^2 \theta \Delta_\theta (\Sigma \Delta_r \dot{\phi} - a\chi eQr)^2}{\chi^2 (\Delta_r - a^2 \sin^2 \theta \Delta_\theta)^2} \right] \\ &= (\Delta_r - a^2 \sin^2 \theta \Delta_\theta) \left(\mu \Sigma - \frac{\Sigma^2 \dot{r}^2}{\Delta_r} - \frac{\Sigma^2 \dot{\theta}^2}{\Delta_\theta} \right) + \frac{\sin^2 \theta \Delta_\theta (\Sigma \Delta_r \dot{\phi} - a\chi eQr)^2}{\chi^2 (\Delta_r - a^2 \sin^2 \theta \Delta_\theta)} \left(\frac{a^2 \sin^2 \theta \Delta_\theta}{\Delta_r} - 1 \right) \\ &\quad + \frac{eQr}{\Delta_r} \left(eQr(\Delta_r - a^2 \sin^2 \theta \Delta_\theta) - \frac{2a \sin^2 \theta \Delta_\theta}{\chi} (\Sigma \Delta_r \dot{\phi} - a\chi eQr) \right) \\ &= (\Delta_r - a^2 \sin^2 \theta \Delta_\theta) \left(\mu \Sigma - \frac{\Sigma^2 \dot{r}^2}{\Delta_r} - \frac{\Sigma^2 \dot{\theta}^2}{\Delta_\theta} \right) - \frac{\Sigma^2 \sin^2 \theta \Delta_r \Delta_\theta \dot{\phi}^2}{\chi^2} + e^2 Q^2 r^2. \end{aligned}$$

Therefore, the positive solution E of $\alpha_i E^i = 0$ reads

$$E = -\frac{\alpha_1}{2\alpha_2} + \sqrt{\frac{\alpha_1^2}{4\alpha_2^2} - \frac{\alpha_0}{\alpha_2}} = -\frac{eQr}{\chi \Sigma} + \sqrt{\frac{a^2 \sin^2 \theta \Delta_\theta - \Delta_r}{\chi^2 \Sigma} \left(\mu - \frac{\Sigma \dot{r}^2}{\Delta_r} - \frac{\Sigma \dot{\theta}^2}{\Delta_\theta} \right) + \frac{\sin^2 \theta \Delta_r \Delta_\theta \dot{\phi}^2}{\chi^4}},$$

and this is exactly the stated formula. \square

Remark 3.2.2. From the set of equations (12), we see that trajectories $\gamma = (t, r, \theta, \phi)$ for which $\theta(\ell_0) = \pi/2$ and $\dot{\theta}(\ell_0) = 0$ for some $\ell_0 \in I$ are confined in the equatorial plane $\theta = \pi/2$. In this case, Carter's constant reduces to $\kappa = \chi^2(aE - L)^2$. Therefore, Carter's constant sometimes refers rather to the constant $C := \kappa - \chi^2(aE - L)^2$ so that $C = 0$ for orbits in the plane $\theta = \pi/2$. More explicitly, the constant C can be written as

$$C = \Delta_\theta p_\theta^2 + \frac{\chi^2 \cos^2 \theta}{\Delta_\theta} \left[\frac{L^2}{\sin^2 \theta} - a^2 \left(E^2 + \frac{\mu \Delta_\theta}{\chi^2} + 3\lambda^2 (aE - L)^2 \right) \right].$$

This expression agrees with the one from [PYYY16, §2.1] when $\lambda \rightarrow 0$.

4. POLAR FORMULATION FOR RNdS TRAJECTORIES AND THE WEIERSTRASS ELLIPTIC FUNCTION

In this entire section, we assume that $a = 0$, that is, we work with the *Reissner-Nordström-(anti) de Sitter (RNdS) metric* which is given, in Boyer-Lindquist (spherical)

coordinates by

$$(RNdS) \quad ds^2 = -\underline{\Delta} dt^2 + \frac{dr^2}{\underline{\Delta}} + r^2(d\theta^2 + \sin^2 \theta d\phi^2)$$

where we let $\underline{\Delta} := \Delta_r/r^2 = 1 - \lambda r^2 - 2M/r + Q^2/r^2$ to lighten the notation. Since this metric is spherically symmetric, the geodesics are planar. Therefore, in order to study geodesics (and to implement them afterwards), we only need to focus on the equatorial ones. More precisely, if we have any geodesic, we may apply a linear rotation (i.e. an element of $1 \times SO(3) \subset \text{Isom}(\mathcal{M} \setminus \{r=0\}, g_{RNdS})$) to force its velocity vector to lie on the equatorial plane, solve the equations and then go back with the inverse rotation.

4.1. Polar geodesic equation. Consider then an equatorial geodesic $\gamma = (t, r, \pi/2, \phi)$ with Hamiltonian μ , energy E and angular momentum L . To simplify our treatment, and as it will be sufficient for the application to the ray-tracing, we will also assume that the charge of the test particle is $e = 0$. The set of equations (12) becomes

$$(16) \quad \begin{cases} \underline{\Delta} \dot{t} = E, \\ r^4 \dot{r}^2 = E^2 r^4 - \Delta_r (L^2 - \mu r^2), \\ r^2 \dot{\phi} = L. \end{cases}$$

From this we see that if $\dot{\phi}$ evaluates to zero somewhere, then $L = 0$ and $\dot{\phi} \equiv 0$ and the motion is then radial. Suppose it is not the case, then $\dot{\phi}$ is a diffeomorphism onto its image and we may express $r = r(\phi)$ as a function of ϕ . We write

$$\left(\frac{dr}{d\phi}\right)^2 = \left(\frac{\dot{r}}{\dot{\phi}}\right)^2 = \left(\frac{r^2 \dot{r}^2}{r^2 \dot{\phi}}\right)^2 = \frac{r^4 \dot{r}^2}{L^2} = \frac{E^2}{L^2} r^4 - \Delta_r \left(1 - \frac{\mu}{L^2} r^2\right)$$

and after calculations,

$$(17) \quad \left(\frac{dr}{d\phi}\right)^2 = -\frac{\lambda\mu}{L^2} r^6 + \left(\lambda + \frac{E^2 + \mu}{L^2}\right) r^4 - \frac{2M\mu}{L^2} r^3 + \left(\frac{Q^2\mu}{L^2} - 1\right) r^2 + 2Mr - Q^2.$$

Now, considering the Binet variable $u := 1/r$, we obtain the equation (from now on, the dot means differentiation with respect to ϕ)

$$(18) \quad \dot{u}^2 = \frac{\dot{r}^2}{r^4} = -\frac{\lambda\mu}{L^2 u^2} + \left(\lambda + \frac{E^2 + \mu}{L^2}\right) - \frac{2M\mu}{L^2} u + \left(\frac{Q^2\mu}{L^2} - 1\right) u^2 + 2Mu^3 - Q^2 u^4.$$

Finally, we can get rid of the square by differentiating again. We find

$$(19) \quad \ddot{u} = \frac{\lambda\mu}{3L^2 u^3} - \frac{M\mu}{L^2} + \left(\frac{Q^2\mu}{L^2} - 1\right) u + 3Mu^2 - 2Q^2 u^3$$

and this equation is much easier to (numerically) solve than the system (15).

4.2. Use of Weierstrass' function \wp for photon orbits. The striking observation that the Weierstrass elliptic function \wp solves the polar equatorial motion equation was first made by Hagihara in [Hag30]. Here, inspired by the method from [GV12, §3.1], we show that we can still use the function \wp to describe null geodesics in the RNdS metric.

In the case of a photon (whose world-line is a null geodesic with $\mu = 0$), the equation (17) reduces to

$$(20) \quad \dot{r}^2 = \left(\lambda + \frac{E^2}{L^2}\right) r^4 - r^2 + 2Mr - Q^2$$

This equation can be further reduced to the Weierstrass equation $\dot{y}^2 = 4y^3 - g_2 y - g_3$ as follows: suppose that $\lambda L^2 + E^2 \geq 0$, then the depressed quartic $(\lambda + E^2/L^2)x^4 - x^2 + 2Mx - Q^2$

has a real root⁷ $\bar{r} \in \mathbb{R}$ and let $\tilde{r} := r - \bar{r}$. We have

$$\begin{aligned} \dot{\tilde{r}}^2 = \dot{r}^2 &= \left(\lambda + \frac{E^2}{L^2} \right) (\tilde{r} + \bar{r})^4 - (\tilde{r} + \bar{r})^2 + 2M(\tilde{r} + \bar{r}) - Q^2 \\ &= \tilde{r} \left[\left(\lambda + \frac{E^2}{L^2} \right) \tilde{r}^3 + 4\bar{r} \left(\lambda + \frac{E^2}{L^2} \right) \tilde{r}^2 + \left(6\bar{r}^2 \left(\lambda + \frac{E^2}{L^2} \right) - 1 \right) \tilde{r} + \left(4\bar{r}^3 \left(\lambda + \frac{E^2}{L^2} \right) - 2\bar{r} + 2M \right) \right] \end{aligned}$$

and considering the new Binet variable $u := 1/\tilde{r} = (r - \bar{r})^{-1}$, we get

$$\dot{u}^2 = \left(\lambda + \frac{E^2}{L^2} \right) + 4\bar{r} \left(\lambda + \frac{E^2}{L^2} \right) u + \left(6\bar{r}^2 \left(\lambda + \frac{E^2}{L^2} \right) - 1 \right) u^2 + \left(4\bar{r}^3 \left(\lambda + \frac{E^2}{L^2} \right) - 2\bar{r} + 2M \right) u^3$$

and it is now straightforward to put this cubic in depressed form and then rewrite it in Weierstrass' form. We summarize the discussion in the following result:

Proposition 4.2.1. *Let $\gamma = (t, r, \pi/2, \phi)$ be a non-circular, non-radial equatorial null geodesic in the RNdS metric, with energy E and angular momentum L . The map $\ell \mapsto \phi(\ell)$ is a diffeomorphism onto its image so that we may re-parametrize γ using ϕ and we abusively denote by r the re-parametrized coordinate $\phi \mapsto r(\phi)$.*

If $\lambda \geq -E^2/L^2$, then we may choose a root $\bar{r} \in \mathbb{R}$ of the quartic

$$(\lambda + E^2/L^2)x^4 - x^2 + 2Mx - Q^2$$

and if we let

$$\begin{cases} \delta = \lambda + E^2/L^2, \\ \gamma = 4\bar{r}\delta, \\ \beta = 6\bar{r}^2\delta - 1, \\ \alpha = 4\bar{r}^3\delta - 2\bar{r} + 2M. \end{cases} \quad \text{as well as} \quad \begin{cases} g_2 := \frac{1}{4} \left(\frac{\beta^2}{3} - \alpha\gamma \right), \\ g_3 := \frac{1}{8} \left(\frac{\alpha\beta\gamma}{6} - \frac{\alpha^2\delta}{2} - \frac{\beta^3}{27} \right), \\ P := \frac{\alpha}{4(r-\bar{r})} + \frac{\beta}{12}, \end{cases}$$

then the function P satisfies the Weierstrass equation

$$\dot{P}^2 = 4P^3 - g_2P - g_3.$$

In other words, if the discriminant $g_2^3 - 27g_3^2 \neq 0$, then the polar radial motion is given by

$$r(\phi) = \bar{r} + \frac{\alpha}{4\wp(\phi) - \beta/3},$$

where $\wp = \wp_{g_2, g_3}$ is the Weierstrass function associated to $(g_2, g_3) \in \mathbb{R}^2$.

Remark 4.2.2. *Differentiating the radial equation from (16) we obtain*

$$\ddot{r} = \frac{2Q^2L^2}{r^6} - \frac{3ML^2}{r^5} + \frac{L^2 - Q^2\mu}{r^4} + \frac{M\mu}{r^3} - \lambda\mu.$$

Fixing an initial value for r and \dot{r} , we obtain a second order Cauchy problem. Hence, if $r : I \rightarrow \mathbb{R}$ is a maximal solution of this problem, then we either have $|r| \rightarrow +\infty$ or $r \rightarrow 0$ on ∂I . This says that ultimately, every geodesic is either always defined (stable orbit), or goes to ∞ (escape path) or dies at the singularity.

Qualitatively, the previous result says that the phase portrait of a generic null RNdS orbit describes (a connected component of) an elliptic curve.

In practice, given a (polar) initial condition $(r_0, \dot{r}_0) := (r(\phi_0), \dot{r}(\phi_0))$, we have to find $z_0 \in \mathbb{C}$ such that $\wp(z_0) = \frac{\alpha}{4(r_0 - \bar{r})} + \frac{\beta}{12}$ and this can be done using the *Carlson integrals* (see [Car95])

$$R_F(x, y, z) := \frac{1}{2} \int_0^\infty \frac{d\zeta}{\sqrt{(\zeta + x)(\zeta + y)(\zeta + z)}}.$$

More precisely, we have the following result:

⁷In practice, we choose \bar{r} with minimal norm so that $\bar{r} = 0$ when $Q = 0$.

Corollary 4.2.3. Fix $(L, E, r_0, \dot{r}_0) \in \mathbb{R}^* \times (\mathbb{R}_+^*)^2 \times \mathbb{R}$ such that $\lambda L^2 + E^2 \geq 0$ and let γ be the unique maximal non-circular, non-radial equatorial null RNdS geodesic with energy E , angular momentum L and such that $r(0) = r_0$ and $\dot{r}(0) = \dot{r}_0$ in polar parametrization $r = r(\phi)$. Recall also the constants $\bar{r}, \alpha, \beta, \gamma, \delta, g_2, g_3$ from Proposition 4.2.1.

If $g_2^3 - 27g_3^2 \neq 0$, then the function r is given (on its definition domain) by

$$r(\phi) = \bar{r} + \frac{\alpha}{4\wp_{g_2, g_3}(z_0 + \phi) - \beta/3}, \quad \text{where } z_0 := R_F(\wp_0 - z_1, \wp_0 - z_2, \wp_0 - z_3) \in \mathbb{C},$$

with $z_{1,2,3} \in \mathbb{C}$ the roots of the Weierstrass cubic $4z^3 - g_2z - g_3$ and $\wp_0 := \frac{\alpha}{4(r_0 - \bar{r})} + \frac{\beta}{12}$.

Numerically, we approach \wp with the Coquereaux-Grossmann-Lautrup algorithm⁸ from [CGL90, §3] and R_F is approximated using the Carlson algorithm from [Car95, §2].

5. MODEL FOR THE ACCRETION DISK

We now detail how we modelled the accretion disk and its radiation. Here, we shall consider a thin steady nearly Keplerian opaque accretion disk contained in the equatorial plane, which is supposed to radiate as a blackbody. For detailed treatments of accretion disks, we refer to [Pri81] and [Spr95].

5.1. Angular velocity of circular massive orbits. First, we have to find the angular velocity of a circular equatorial orbit. This is done in the following result:

Proposition 5.1.1. Let $\gamma = (t, r, \theta, \phi) : I \rightarrow \mathcal{M}$ be a geodesic such that $\theta \equiv \pi/2$ and $\dot{r} = 0$. Then, the angular velocity $\omega := \dot{\phi}/\dot{t}$ is given by

$$\omega = \frac{1}{a + r^2/\rho},$$

where $\rho := \sqrt{-\lambda r^4 + Mr - Q^2}$.

Proof. Consider the Lagrangian

$$\mathcal{L} = \frac{1}{2}g_{\mu\nu}\dot{\gamma}^\mu\dot{\gamma}^\nu = p_\mu\dot{\gamma}^\mu - \mathcal{H}(\gamma, p).$$

Since $\dot{r} = 0$, we have $\frac{\partial \mathcal{L}}{\partial \dot{r}} = 0$ and the radial Euler-Lagrange equation is

$$0 = 2 \frac{d}{d\ell} \left(\frac{\partial \mathcal{L}}{\partial \dot{r}} \right) = 2 \frac{\partial \mathcal{L}}{\partial r} = \frac{\partial g_{tt}}{\partial r} \dot{t}^2 + 2 \frac{\partial g_{t\phi}}{\partial r} \dot{t} \dot{\phi} + \frac{\partial g_{\phi\phi}}{\partial r} \dot{\phi}^2$$

and setting $\omega := \dot{\phi}/\dot{t}$, this is equivalent to

$$g_{tt,r} + 2g_{t\phi,r}\omega + g_{\phi\phi,r}\omega^2 = 0$$

and computing the derivatives, we obtain

$$\begin{aligned} g_{tt,r} + 2g_{t\phi,r}\omega + g_{\phi\phi,r}\omega^2 &= 0 \\ \iff \frac{2(r^4 + a^2\Delta_r - a^4) - a^2r\Delta'_r}{\chi^2r^3}\omega^2 + \frac{2a(r\Delta'_r + 2(a^2 - \Delta_r))}{\chi^2r^3}\omega + \frac{2(\Delta_r - a^2) - r\Delta'_r}{\chi^2r^3} &= 0 \\ \iff (\chi r^4 - a^2(Mr + Q^2))\omega^2 - 2a(\lambda r^4 - Mr + Q^2)\omega + \lambda r^4 - Mr + Q^2 &= 0 \\ \iff \omega = \frac{a\rho^2 \pm r^2\rho}{a^2\rho^2 - r^4} = \rho \frac{a\rho \pm r^2}{(a\rho - r^2)(a\rho + r^2)} = \frac{\rho}{a\rho \mp r^2} \end{aligned}$$

But when $\lambda = a = Q = 0$, we must find $\omega = +\sqrt{M/r^3}$ and thus the above sign is a plus. \square

⁸based on the duplication formula and the Laurent expansion of \wp at 0

5.2. Blackbody radiation temperature and brightness. As mentioned above, we assume that the matter in the accretion disk radiates as a blackbody. To compute its surface temperature $T_s = T_s(r)$, we use the *Shakura-Sunyaev formula* (see [SS73, §2a] or [Spr95, formula (26)]). In SI units, it reads

$$(21) \quad \sigma_B T_s(r)^4 = \frac{3GM\dot{M}}{8\pi r^3} \left(1 - \sqrt{\frac{r_{\text{int}}}{r}}\right),$$

where r_{int} is the interior radius of the disk, \dot{M} is the *accretion rate* of matter into the disk and σ_B is the Stefan-Boltzmann constant.

Now, for the brightness, we use Planck's law (h is Planck's constant and k_B is Boltzmann's constant)

$$B_\lambda(T) = \frac{2hc^2}{\lambda^5} \frac{1}{e^{\frac{hc}{k_B\lambda T}} - 1}$$

coupled with the Wien law $\lambda = b/T$, where b is Wien's displacement constant. This yields, after evaluating the constants,

$$B(r) := B_{b/T}(T_s(r)) = \frac{2hc^2}{b^5} \frac{T^5}{e^{\frac{hc}{k_B b}} - 1} \approx 4.086 \cdot 10^{-6} \times T^5.$$

This is the value by which we shall multiply the pixel's RGB triple corresponding to the temperature T_s , according to the conversion table by M. Charity⁹. However, it turns out that implementing these values gives an over-bright disk, hence we found useful to rescale the brightness by 10^{-15} so that $B(r) \approx 4.086 \cdot 10^{-21} \times T^5$. Then, the user is invited to give a value $B_0 \geq 0$, typically $B_0 \leq 10^4$, so that the disk becomes visible as changing the inner (outer) radius or the accretion rate dramatically affects the brightness. The rescaled brightness is then $\tilde{B}(r) = B_0 T^5 \times 4.086 \cdot 10^{-21}$. If $B_0 = 0$ is chosen, then the formula above for $B(r)$ is ignored and a linear scaling of brightness is taken, from the outer radius to the inner one.

5.3. Gravitational redshift and Doppler effect. Last, we have to take the Doppler effect and gravitational redshift into account for the temperature and the brightness, as we deal with relativistic speeds and strong gravitational fields. More precisely, we will rescale the temperature and brightness by factors $\alpha_{\text{Grav}}^{-1} = (1 + z_{\text{Grav}})^{-1}$ and $\alpha_{\text{Dop}}^{-1} = (1 + z_{\text{Dop}})^{-1}$ corresponding to the gravitational and Doppler shifts, respectively.

The gravitational redshift is easily computed from the matrix $(g_{\mu\nu})$. Indeed, for a stationary observer (a test particle with $\dot{r} = \dot{\theta} = \dot{\phi} = 0$), the KNdS metric reduces to $ds^2 = -c^2 d\tau^2 = g_{tt} c^2 dt^2$, where τ is the proper time of the observer. Therefore, the gravitational redshift for such an observer is simply given by

$$\alpha_{\text{Grav}} = \frac{dt}{d\tau} = \frac{1}{\sqrt{-g_{tt}}} = \chi \sqrt{\frac{\Sigma}{\Delta_r - a^2 \sin^2 \theta \Delta_\theta}}.$$

Now, the Doppler shift is derived as follows. Consider a circular massive orbit with constant radius r and angle $\phi = \phi(\ell)$ photon path leaving the point $(t, r, \pi/2, \phi)$ with angle ϑ with respect to the four velocity $l^\mu = (\dot{t}, 0, 0, \dot{\phi})$. Following [LL80, §48], the Doppler shift is given (in natural units) by

$$\alpha_{\text{Dop}} = \frac{1 - v \cos \vartheta}{\sqrt{1 - v^2}},$$

where $v = \sqrt{r^2 + a^2} \omega$ is the velocity of the circular orbit which reads, using Proposition 5.1.1,

$$v = \frac{\sqrt{r^2 + a^2}}{a + \frac{r^2}{\sqrt{-\lambda r^4 + Mr - Q^2}}}.$$

⁹<http://www.vendian.org/mncharity/dir3/blackbody/>

6. IMPLEMENTATION AND COMPARISON OF THE METHODS

In this final section, we give some details on the Scilab functions we created to solve the geodesic equations and to draw the shadow of a KNdS black hole, with an accretion disk. The functions are designed to allow the user to tune parameters (cosmological constant mass, charge, angular momentum, accretion rate, brightness...) as wanted and to draw a shadow accordingly. The full scripts and documentation can be found at https://github.com/arthur-garnier/knds_orbits_and_shadows.git.

First, as the cosmological constant makes the computations heavier and as it is very likely to be very small¹⁰, we added versions of our programs for the Kerr–Newman case (i.e. for $\Lambda = 0$). The resulting functions are combined in single `.sci`. In all our programs, we systematically rescale the initial data so that $G = c = M = 4\pi\epsilon_0 = 1$ and go back to SI units after computations.

The programs `formulations.sci` and `geodesics.sci` are intended to solve the geodesic equations. The first one is simply a library of useful functions, such as the conversion between Cartesian and Boyer-Lindquist coordinates (orbits are drawn using Cartesian coordinates), the (inverse and derivatives of the) metric matrices, Christoffel symbols, etc. The second one is the solver itself. It takes as input the cosmological constant, the three parameters of the black hole, the mass of the particle (0 or 1), the discretized affine parameter (maximal value and step-size) and the initial conditions of the geodesic, in Boyer-Lindquist coordinates. It also lets the user choose between the different integration methods we discussed above, as well as the method to use in the `ode` command¹¹. As output, it yields the trajectory in BL coordinates and the Hamiltonian along the trajectory (the values of (r, θ, ϕ) and of \mathcal{H} at each node).

6.1. Shadowing and the backward ray tracing method. The method we use to create the shadow of the black hole is quite standard: the *backward ray tracing*. For a detailed and illustrated explanation of this method, we refer to [VALPO22]. The function that ray-traces the black hole is `shadow.sci`; it takes as input the parameters of the black hole and the cosmological constant, the image to use for the shadowing and the accretion data¹². Though doable with any integration method, we used the Carter equations for `shadow.sci`, as it is by far the fastest method available (see Section 6.3).

The basic idea is as follows: consider a static point in the KNdS space-time, far from the center, representing the “eye” of our observer. Consider also a screen between our observer and the black hole, orthogonal to the segment joining the center and the observer. The celestial sphere emits light in every direction and some of it will eventually reach the observer, passing through the screen and the point where it hits the screen gives the pixel to draw at this point, depending on where it left the celestial sphere. However, as light will not propagate in straight lines, it is hard to know which ray will cross the screen in advance.

Therefore, we work backwards: suppose the observer emits light in every direction and keep only those rays that hit the screen at some point. As we are far from the source, we assume that light travels in straight lines between the camera and the screen. Then, we let the light ray trace backward in time and see where it eventually lands (actually, where it came from): if it dies in the black hole, no pixel is displayed on the screen and if it crosses the celestial sphere, then the pixel is coloured in accordance with where it touches the sphere.

This amounts to say that, first, we consider an artificial celestial hemisphere on which we project our original image, seeing it as a portion of its tangent plane which is parallel to our

¹⁰According to [Col20, §3.2], the physical value of Λ should be $0 < \Lambda = (1.090 \pm 0.029) \cdot 10^{-52} \text{m}^{-2}$ in SI units.

¹¹such as RK4, RK45, BDF, Adams... see https://help.scilab.org/docs/6.1.1/en_US/ode.html

¹²inner and outer radii, accretion rate, angle of view (from the equatorial plane) and brightness. But it also allows one to force the temperature at extremal radii and to choose between the different shifts (gravitational, Doppler, both, none) described in Section 5. For more details, see https://github.com/arthur-garnier/knds_orbits_and_shadows.git.

screen (and on the other side of the black hole). As a projection, we choose an equatorial variant of the *azimuthal equidistant projection*, which respects the distance to the central point of the tangent plane and directions from the center, but other types are possible (e.g. Aitoff, Hammer...); we just need a differentiable and fast-to-compute method, for which the area near the center is not too much deformed. The celestial hemisphere now is tiled by coloured pixels. Next, for each pixel of the screen, we consider the null geodesic starting at this point and with velocity given by the condition that it comes from the point observer. Then, we solve the geodesic equations (backward in time) and we see if the ray ends in (came from) the black hole or touches the sphere somewhere. If so, the RGB value of the pixel on the screen is then given by the value of the landing pixel on the sphere. Once every pixel of the screen has been worked out, we display it. We illustrate this in Figure 3.

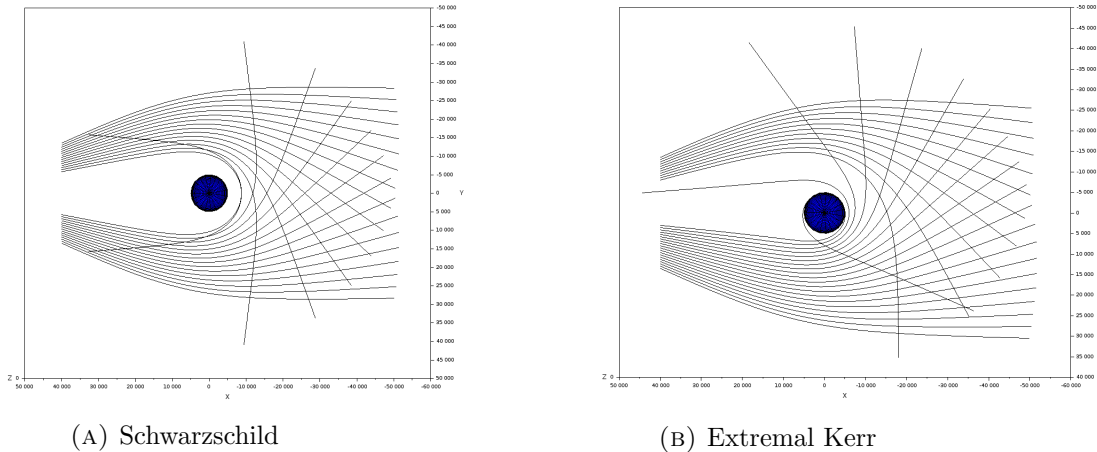


FIGURE 1. A pencil of equatorial rays near a black hole.

Concerning the accretion disk, we simply interpolate the plane $\{\theta = \pi/2\}$: if the geodesic ray hits the plane (up to some fixed threshold) at a point whose radius r is between the extremal radii of the disk, then we compute the radiation temperature at this point, as well as the gravitational and Doppler effects described in Section 5. We then give the corresponding colors and brightness to the associated pixel on the screen.

It is to be mentioned that, technically, we rather project the landing (starting) point of each geodesic ray on the sphere to the tangent plane, rather than the contrary. This is because we first need to know the maximal coordinates on the plane we may reach in this way, in order to rescale the original image properly, as it is hard to guess in advance what the range of the image on the plane should be. More on this will be said in Section 6.2. Therefore, we look for a projection from the sphere to some tangent plane.

The “equatorial azimuthal” equidistant projection we use is as follows: in \mathbb{R}^3 , take the unit sphere \mathbb{S}^2 and let $T_p\mathbb{S}^2$ be its tangent space at the point $p := (1, 0, 0)$. Consider a point $q := (x, y, z)$ on the punctured sphere $\mathbb{S}^2 \setminus \{-p\}$. There is a unique minimal geodesic (for the round metric on \mathbb{S}^2 and parametrized by arc-length) γ_q from p to q and let $\vec{v} := \dot{\gamma}_q(0) \in T_p\mathbb{S}^2$ be its unitary initial velocity. Then, the projected point $\pi(q) \in T_p\mathbb{S}^2$ is given by

$$(22) \quad \begin{array}{ccc} \mathbb{S}^2 \setminus \{-p\} & \xrightarrow{\pi} & T_p\mathbb{S}^2 \\ q & \longmapsto & p + \ell(\gamma_q)\vec{v} \end{array}$$

This is indeed at Euclidean distance $\ell(\gamma_q)\|\vec{v}\| = d_{\mathbb{S}^2}(p, q)$ from p . As γ_q is given by $\gamma_q(s) = \cos(s)p + \sin(s)q^\perp$, where $\{p, q^\perp\}$ is the Gram-Schmidt orthonormalization of the basis $\{p, q\}$ of the unique linear hyperplane containing p and q . We obtain $\pi(p) = (1, \varrho \cos \vartheta, \varrho \sin \vartheta)$, with $\varrho = \arctan2(\sqrt{y^2 + z^2}, x)$ and $\vartheta = \arctan2(z, y)$, where $\arctan2$ is the arctangent function with two arguments. The projected hemisphere is displayed in Figure 2.

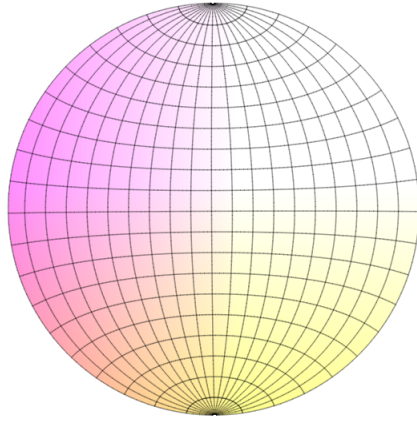


FIGURE 2. The hemisphere projected using the map π from (22).

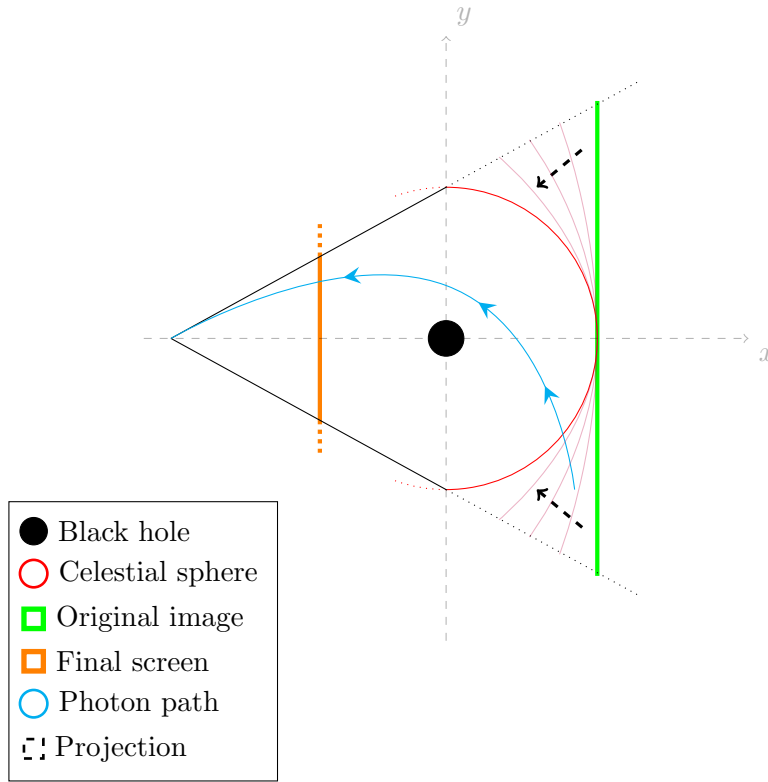


FIGURE 3. Schematics of our shadowing method (in the xy -plane).

All this requires a Scilab package for processing images. For instance, the package IPCV 4.1.2 for Scilab 6.1.1 is quite fine¹³. The command `imread` loads an image (`.jpg`, `.png`, etc) with $N \times M$ pixels and encodes it as an $N \times M \times 3$ hypermatrix with, for each $(i, j) \in \{0, \dots, N\} \times \{0, \dots, M\}$, the three RGB values of the pixels in position (i, j) and this is particularly suitable for our purpose. Then, we produce our pixels for the shadowed image as described above and put them in a similar $N \times M \times 3$ hypermatrix, which we can display as an image using the command `imshow`.

¹³See <https://atoms.scilab.org/toolboxes/IPCV> and <https://ipcv.scilab-academy.com>

6.2. Optimization of the shadowing process with \wp . As mentioned in Section 6.1, in order to rescale the original image properly, we first need to compute the geodesic ray for each pixel of the receiving screen and see where (if ever) it lands on the celestial sphere. Then, we project the landing points on the plane using the map π and we scale the image so that it fits in the resulting “rectangle” on the plane. Thus, we have to make at least two loops on the pixels: the first one to compute the geodesics and store the starting and the (projected) landing points, then we scale the image and then we make a second loop to attribute an RGB value for each pixel on the screen, depending on which pixel it reaches on the rescaled image. This second loop slows the program down by an order of magnitude.

However, we can get rid of this difficulty using the Weierstrass function, at the cost of a small inaccuracy on the final picture. The idea is the following: consider a RNdS (non-rotating) black hole. The associated metric is spherically symmetric and, as described in Proposition 4.2.1 and Corollary 4.2.3, a photon path in the RNdS metric is explicitly described in terms of the Weierstrass \wp function, for which efficient algorithms ([CGL90] and [Car95]) exist to approach it and its inverse. Moreover, because of the symmetry, we don’t have to compute every geodesic: given an initial datum, use a linear rotation to bring the initial velocity (and hence the full orbit) in the plane $\{\theta = \pi/2\}$. Then, we give values to the various constants involved in the expression of the polar radial geodesic and, instead of computing the full orbit, we simply solve the equation $r = r_{\mathbb{S}}$ where $r_{\mathbb{S}}$ is the radius of the imaginary celestial sphere. This can be done rather easily, precisely and quickly: we compute some values until we cross the sphere and the first such point is used as an initial value for the Newton method¹⁴. Then we rotate the result back and find our landing pixel. Moreover, the computation of \wp and the related constants is required only for a quarter of the pixels, the other ones being obtained by symmetry. Thus, no full orbit calculation nor ODE solving is required and this makes the resulting function `shadow-wp.sci` quite fast.

This trick can also be used for the general function: first, we set the rotation parameter to 0 and compute, using \wp and the method above, the maximal coordinates a pixel can reach on the tangent plane to the celestial sphere. Then, the only loop we have to do on the pixels is the one that effectively compute the geodesics using an Adams method on the system (3.1.2) and attributes the RGB values to the pixels. The resulting function is `shadow-fast.sci`.

6.3. Comparison of the accuracy and execution time of the integrators. We can now compare the different formulations and schemes. Concerning the accuracy, we compare the conservation of the Hamiltonian and Carter constant along trajectories. For the execution times, we will shadow a KNdS black hole in low resolutions, as some of the methods are quite long. We shall observe that the fastest and most accurate method is, as one could expect, the Carter equations. In the case of a RNdS black hole, it is of course the analytic method using \wp which is the fastest. Next, we illustrate the advantages of the Weierstrass trick for accelerating the general shadowing.

Consider a massive orbit ($\mu = -1$) with $(r_0, \theta_0, \phi_0, \dot{r}_0, \dot{\theta}_0, \dot{\phi}_0) = (12.26, \pi/2, 0, 0, 0.014, 0.019)$ in a KNdS space-time with parameters $M = 3.367 \cdot 10^{30}$, $a = 0.75$, $Q = 0.5$ and $\Lambda = 3 \cdot 10^{-4}$. This is a non-planar orbit so the Carter constant is not 0. The orbit is depicted in Figure 4. The evolution of the Hamiltonian and Carter constant are depicted in Figures 5 and 6.

To be more quantitative, the maximal deviations and execution times for each method are summarized in the Table 1. This table shows that the two symplectic Euler schemes are comparable in terms of conservation, but the q -implicit one is, as expected, around twice as fast as the other one. The implicit Störmer-Verlet scheme is far more efficient than the Verlet scheme, but it is also the slowest method. The Euler-Lagrange formulation is rather fast, but leaves the Hamiltonian far from being constant. The Hamilton formulation is very efficient and rather fast, and seems to be the most reasonable method, except for the Carter

¹⁴We also use this procedure for the accretion disk, rather than a naive interpolation.

equations 15. This is definitely the fastest and most efficient method we have, almost three times faster than any other one.

In Figure 7, we display some remarkable planar leaf-orbits. These all have $\theta_0 = \pi/2$ and $\phi_0 = \dot{r}_0 = \dot{\theta}_0 = 0$. The parameters of the space-time are the same as above.

In order to compare the different methods of integration regarding the shadowing process, we make several shadows of the same black hole, using the base picture displayed in Figure 8. To simplify, we take $\Lambda = 0$ and the parameters of the black hole are set to $M = 4.72 \cdot 10^{30}$, $a = 0.75$ and $Q = 0.5$. The images have a resolution of 72×72 and are depicted in Figure 9. The corresponding execution times are in Table 2. We can see that all the symplectic schemes present a singularity at the rotation axis.

We may also see how the execution times grow with the number of pixels. As the answer is pretty clear, we only made the computation for the same image and with resolutions from 10×10 to 20×20 pixels. The resulting graph (in log-log scale) is in Figure 10. As expected, the best method is, by far, the Carter equations (numerically integrated with the Adams methods from [Hin80]). It should be mentioned that the function we used to draw these shadows is longer than a program using a specific method such as `shadow.sci`, since it is designed to work with all methods at once.

Finally, we compare the Carter method with the Weierstrass one in the case $a = 0$ and see how using \wp can reduce the time of shadowing a KNdS black hole. We shadow a Kerr–Newman space-time with $M = 4.72 \cdot 10^{30}$, $a = 0.75$ and $Q = 0.5$, using the two methods (with and without \wp). We can also set $a = 0$ and do the same shadow using the specific function `shadow-wp.sci`. The result is as in Figure 11. We see that the function `shadow-fast.sci` is much faster than `shadow.sci`: in log-log scale, the slope of the regression line is 2.46 (standard deviation 3%) for `shadow.sci` and 2.04 (same deviation) for `shadow-fast.sci`. On the other hand, the slope for \wp alone is 1.82 (deviation 6%). The difference in the images from `shadow.sci` and `shadow-fast.sci` becomes negligible with a relatively high number of pixels. Using a resolution of 144×144 , we obtain the images in Figure 12.

Every computation was made on a 12-core 2.60 GHz CPU with 16 Go of RAM. The pictures we used for shadowing (the Milky Way and Hubble’s deep field) are from the NASA.

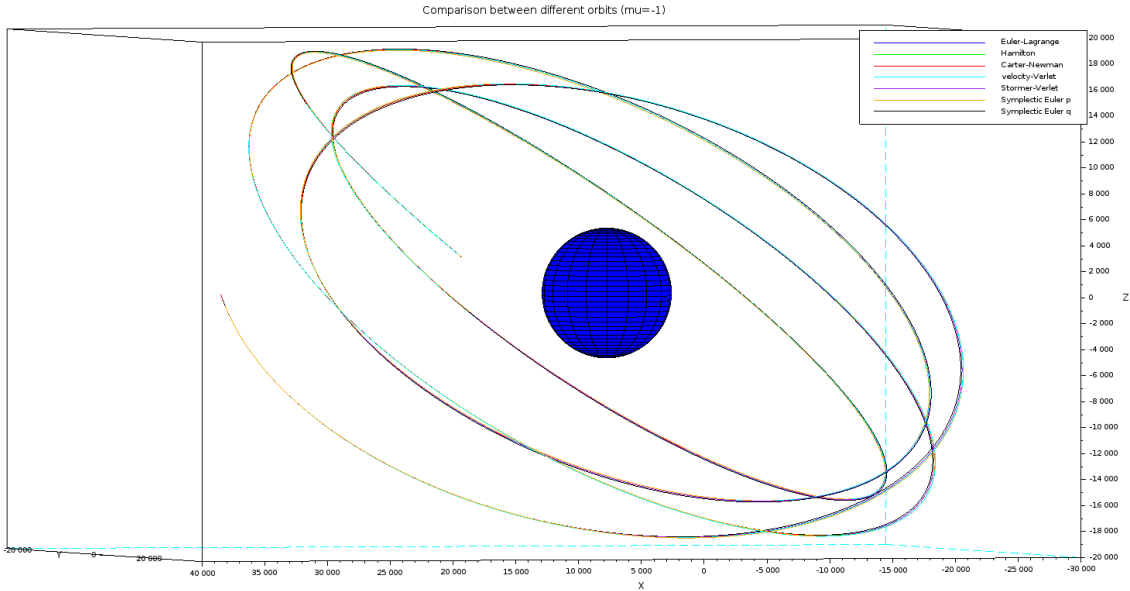


FIGURE 4. A non-planar prograde orbit around a KNdS black hole with $a = 0.75$, $Q = 0.5$ and $\Lambda = 3 \cdot 10^{-4}$. The central sphere represents the Schwarzschild radius.

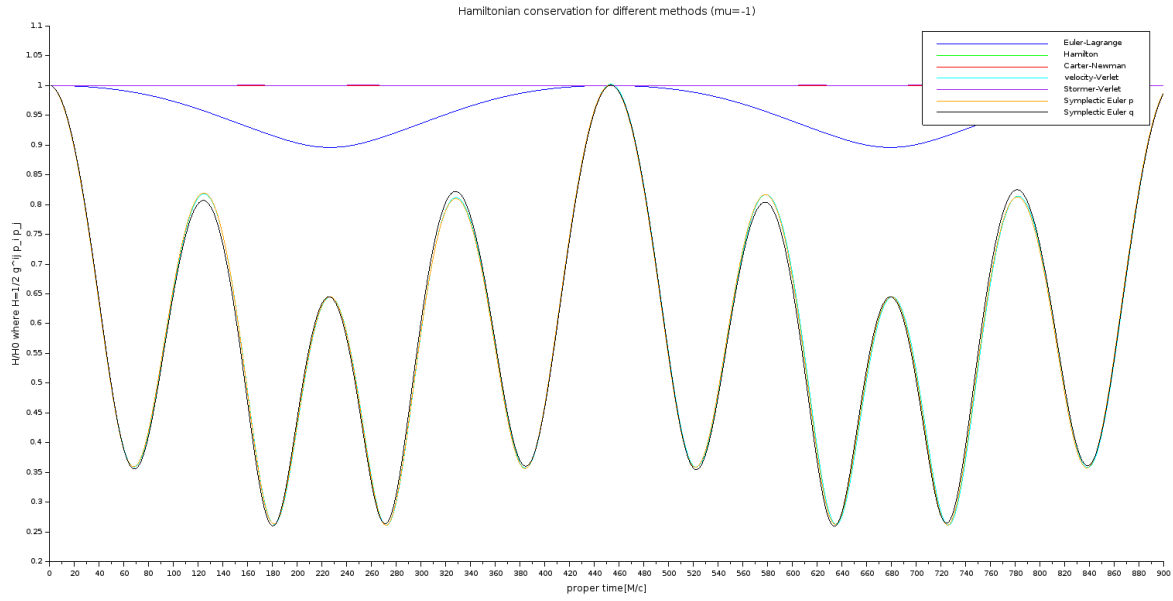


FIGURE 5. Hamiltonian evolution.

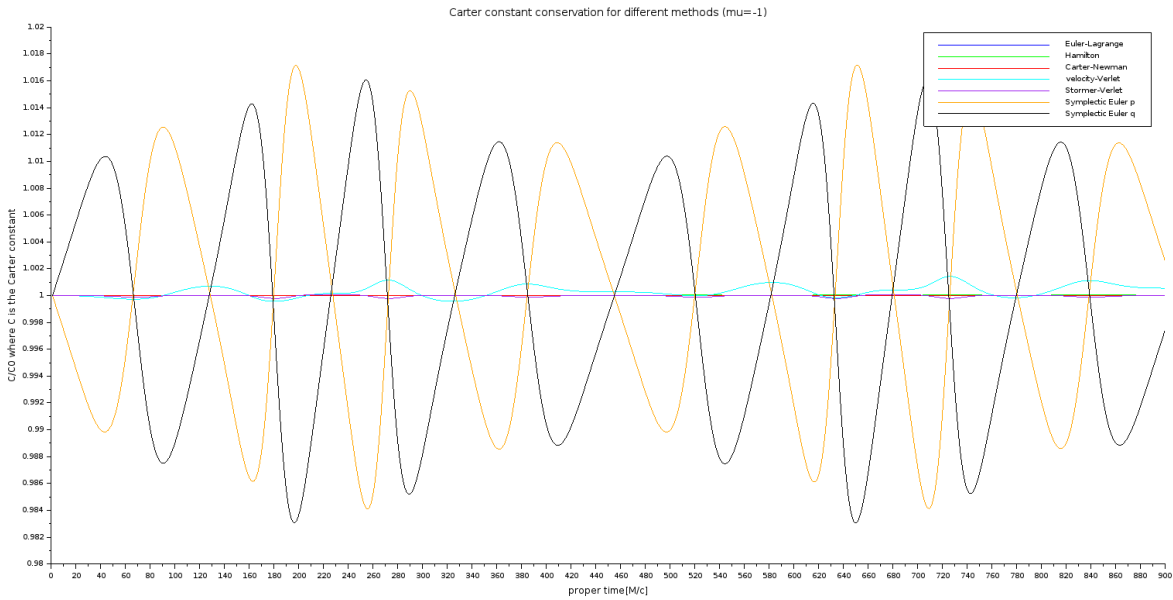


FIGURE 6. Carter's constant evolution.

	Max deviation on \mathcal{H}	Max deviation on C	Execution time (sec)
Euler-Lagrange	0.104	$2.56 \cdot 10^{-5}$	0.316
Hamilton	$8 \cdot 10^{-7}$	$3.95 \cdot 10^{-5}$	0.363
Carter	$4 \cdot 10^{-7}$	$2.9 \cdot 10^{-5}$	0.134
Velocity-Verlet	0.739	$1.34 \cdot 10^{-3}$	0.312
Störmer-Verlet	$6.87 \cdot 10^{-4}$	$1.91 \cdot 10^{-4}$	0.81
p -implicit Euler	0.739	$1.62 \cdot 10^{-2}$	0.715
q -implicit Euler	0.740	$1.6 \cdot 10^{-2}$	0.423

TABLE 1. Comparison of the methods.

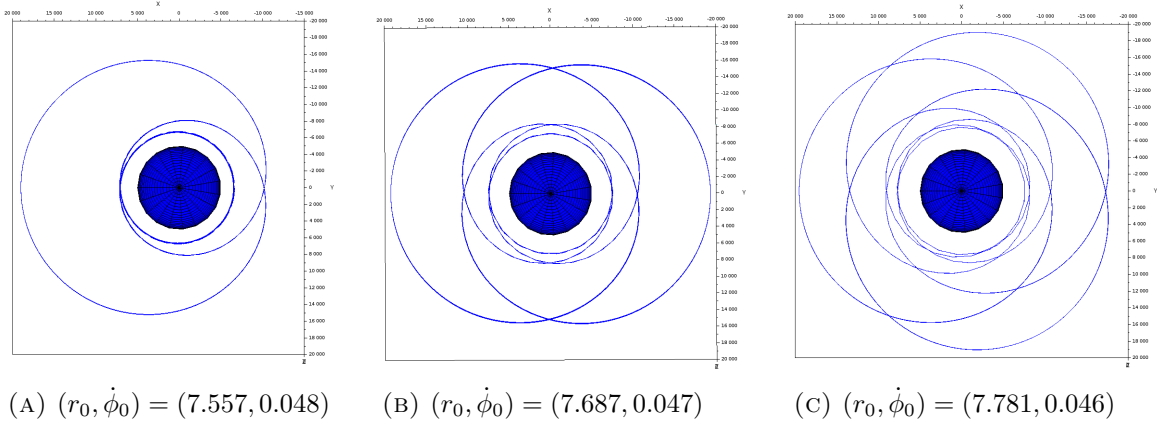


FIGURE 7. Orbits with one, two and three leaves (unit-less initial data).



FIGURE 8. The base picture.

	Euler-Lagrange	Hamilton	Carter	Velocity-Verlet	Störmer-Verlet	q -implicit Euler
Times (sec)	843.04	602.77	134.91	409.33	1398.03	658.66

TABLE 2. Execution times for the shadows of Figure 9.

6.4. Some illustrations and a simulation of M87*. We finish by giving some figures using `shadow-fast.sci` and `shadow-wp.sci`. Besides, we illustrate the model for the accretion disk described in Section 5 and we include a simulation of the M87 black hole, using the data from [GVW⁺21].

In each case, we label Figure with the space-time parameters, resolution `pix` and average execution time t_e . We also indicate the inclination angle i (from the symmetry axis), the inner (resp. outer) radius r_i (resp. r_e) of the accretion disk and the accretion rate \dot{M} used in the equation (21) as well as the brightness scaling B_0 .

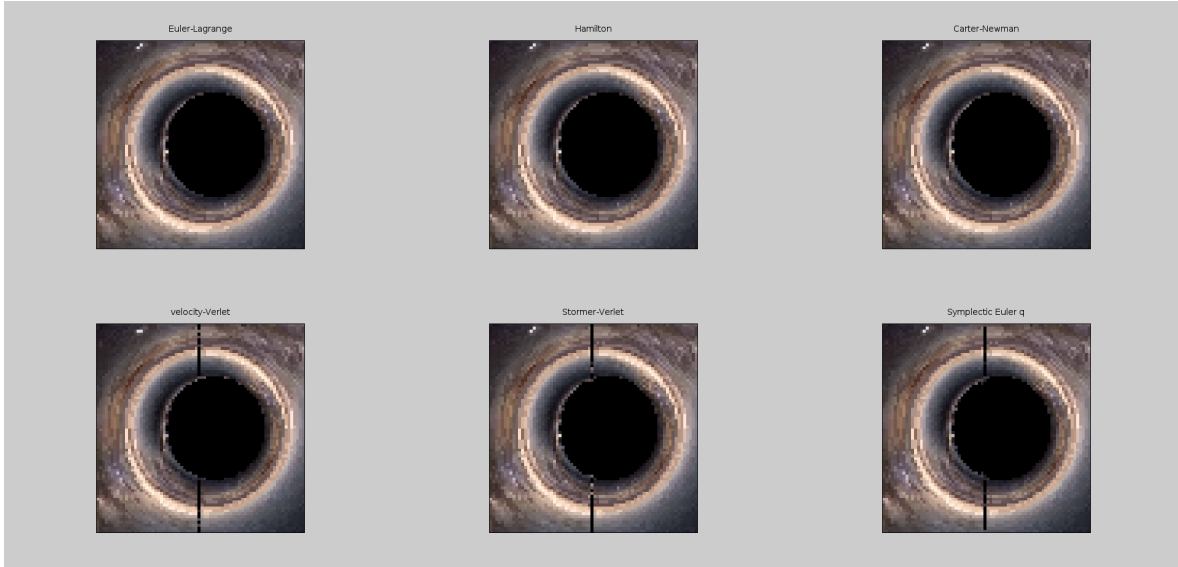
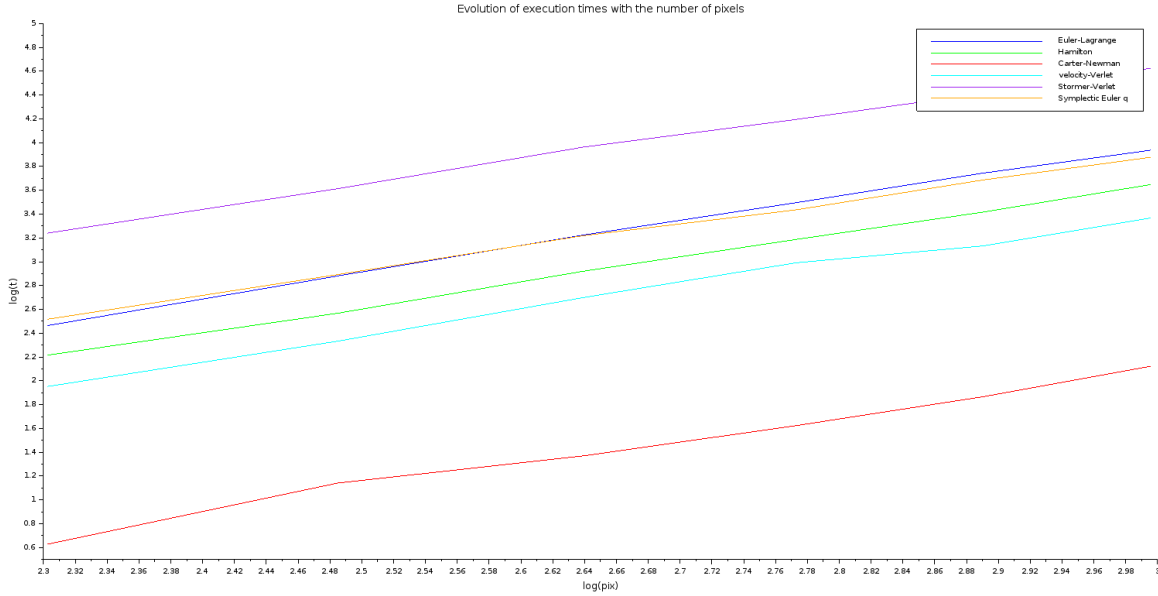

 FIGURE 9. Shadows obtained with the different methods (72×72).


FIGURE 10. Growth of execution times with the number of pixels to shadow.

Except for the simulation of M87*, we set the mass to twice the Solar mass: $M = 4 \cdot 10^{30} \approx 2M_{\odot}$. This is because of the choice we made in our code, but one may of course renormalize lengths. The pictures for which $a = 0$ were made using the Weierstrass form and not Carter's equations.

Finally, concerning the modelling of the M87 black hole, inspired by [GVW⁺21], the black hole and accretion parameters are in the Table 3. We rescaled the mass so that it fits with our code where the typical mass is around twice the solar mass. Next, as the physical value $\Lambda \sim 10^{-52} \text{m}^{-2}$ will not visibly affect the picture, we choose to take $\Lambda = 0$. Also, we changed some values, marked with a star, which we had to arbitrarily choose (or change from the reference) for the implementation. Besides, we included the combination of the gravitational and Doppler effects in the computation. The result is depicted in Figure 19. To make the photon ring even more visible, we also took another picture of the same black hole. The only changed values are $r_i = 5.82M$, $r_e = 16M$, $\dot{M} = 10$, $B_0 = 5000$.

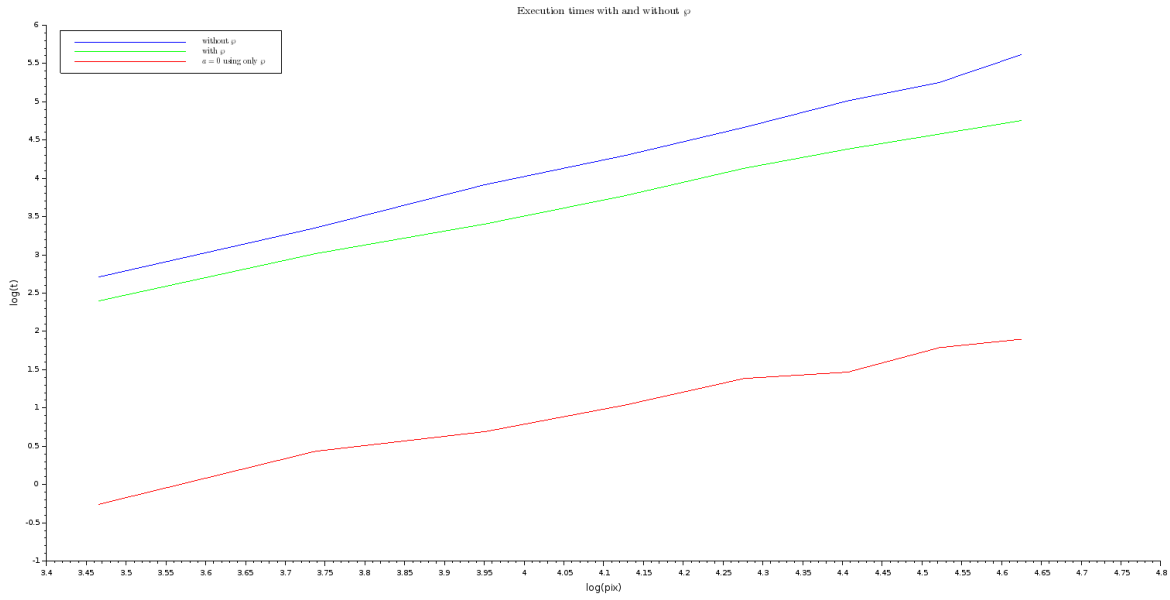
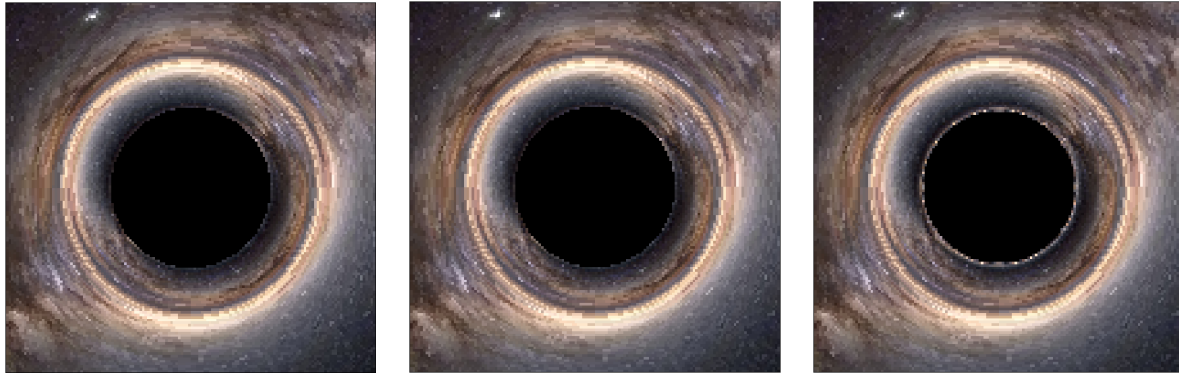


FIGURE 11. How using φ can accelerate the computations.

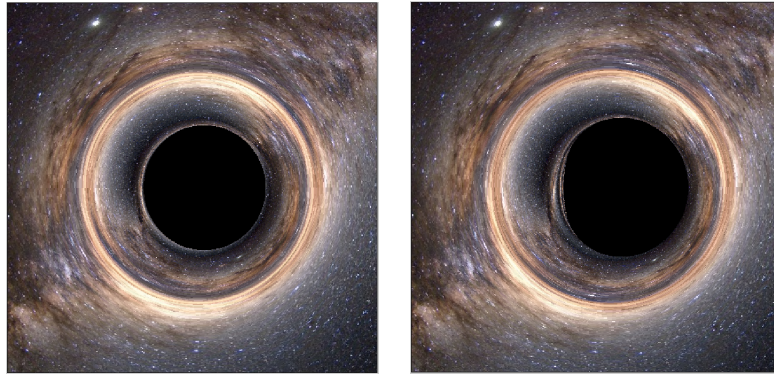


(A) shadow.sci (686 s). (B) shadow-fast.sci (200 s). (C) shadow-wp.sci (14 s).

FIGURE 12. Comparison of the results of shadow.sci, shadow-fast.sci and shadow-wp.sci on a 144×144 picture.

Parameter	Value
Mass*	$M = 1.5M_{\odot}$ (value in [GVW ⁺ 21]: $M \approx 6.2 \cdot 10^9 M_{\odot}$)
Charge	$Q = 0$
Kerr parameter	$a = 0.8$
Accretion rate*	$\dot{M} = 3$
Inner radius	$r_i = 2.91M$
Outer radius*	$r_e = 10M$
Brightness rescaling	$B_0 = 3800$
Angle from symmetry axis	$i = 160^{\circ}$
Resolution	720p

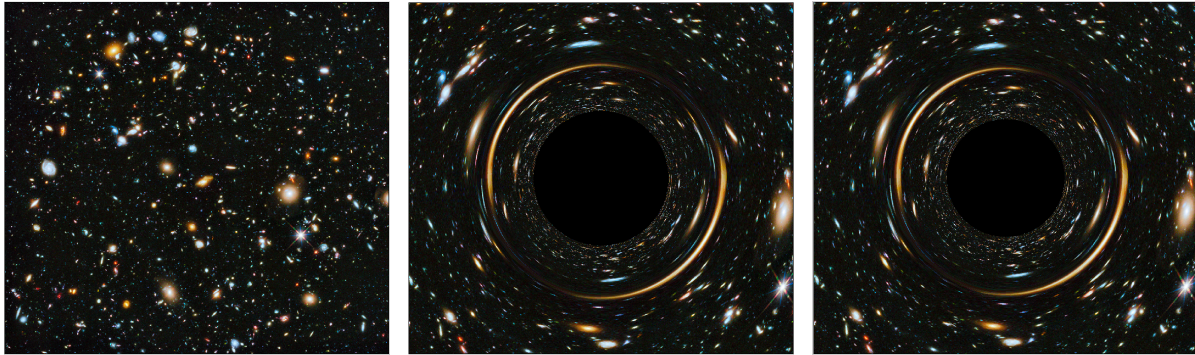
TABLE 3. Parameters for the picture of M87* and its accretion disk.



(A) $a = 0.4$

(B) $a = 0.9$

FIGURE 13. $\Lambda = 0$, $Q = 0.8$; $\text{pix} = 480^2$; $t_e \sim 2000s$.

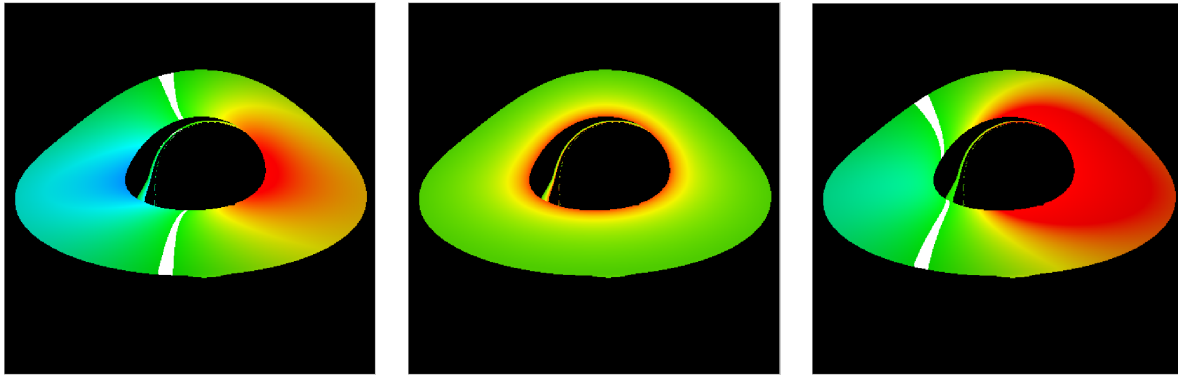


(A) $M = 0$

(B) $Q = 0$

(C) $Q = 0.8$

FIGURE 14. Hubble's field: $\Lambda = a = 0$; $\text{pix} = 1200 \times 1096$; $t_e \sim 3800s$.

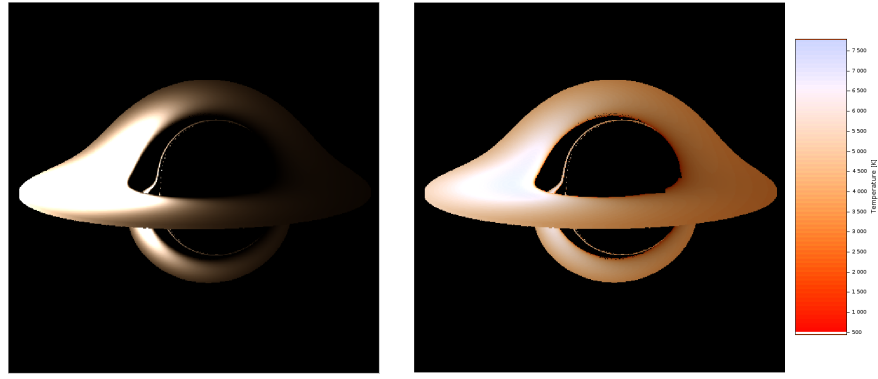


(A) Doppler redshift

(B) Gravitational redshift

(C) Both

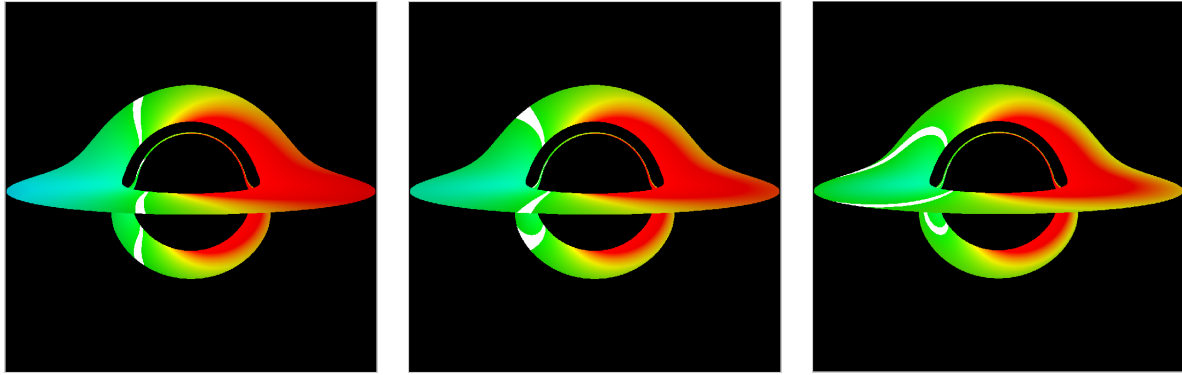
FIGURE 15. $\Lambda = 0$, $a = 0.94$, $Q = 0.8$; $\text{pix} = 480^2$; $t_e \sim 4000s$; $i = 3\pi/8$, $r_i = 4M$, $r_e = 12M$. The white strips correspond to where the shift is negligible.



(A) Radiation temperature with $B_0 = 50$

(B) Radiation temperature with $B_0 = 0$

FIGURE 16. $\Lambda = 0$, $a = 0.94$, $Q = 0.8$; $\text{pix} = 480^2$; $t_e \sim 3000s$; $i = 4\pi/9$, $r_i = 4M$, $r_e = 12M$, $\dot{M} = 90$.

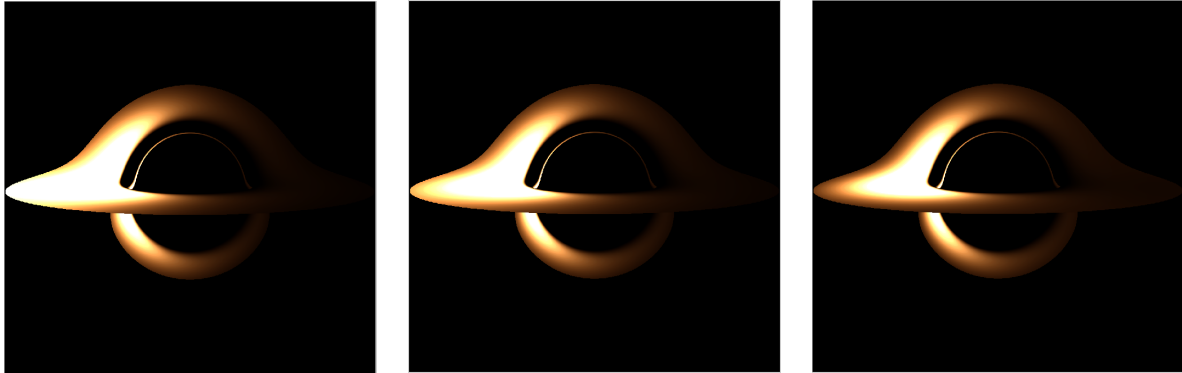


(A) $\Lambda = -10^{-3}$

(B) $\Lambda = 0$

(C) $\Lambda = 10^{-3}$

FIGURE 17. $a = 0$, $Q = 1$; $\text{pix} = 1080^2$; $t_e \sim 4000s$; $i = 13\pi/28$, $r_i = 4M$, $r_e = 12.6M$.

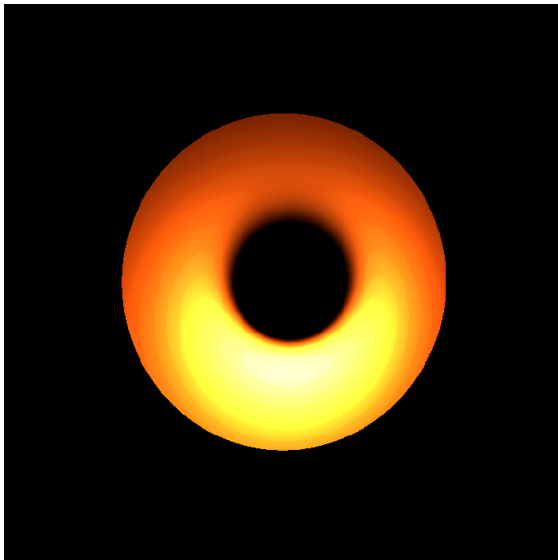


(A) $\Lambda = -10^{-3}$

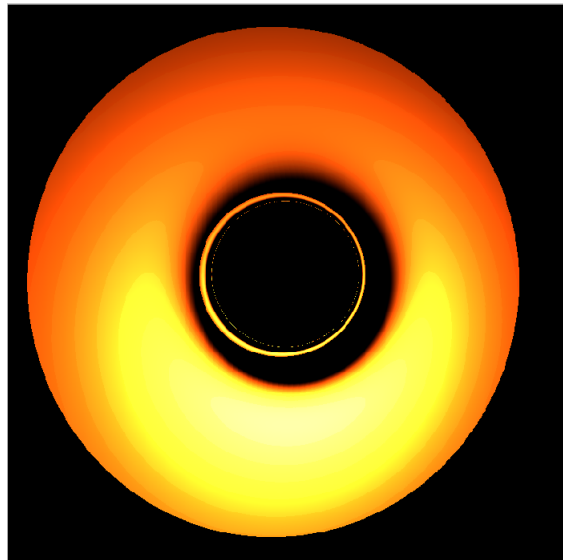
(B) $\Lambda = 0$

(C) $\Lambda = 10^{-3}$

FIGURE 18. $a = 0$, $Q = 1$; $\text{pix} = 1080^2$; $t_e \sim 4000s$; $i = 13\pi/28$, $r_i = 4M$, $r_e = 12.6M$, $\dot{M} = 20$, $B_0 = 300$.

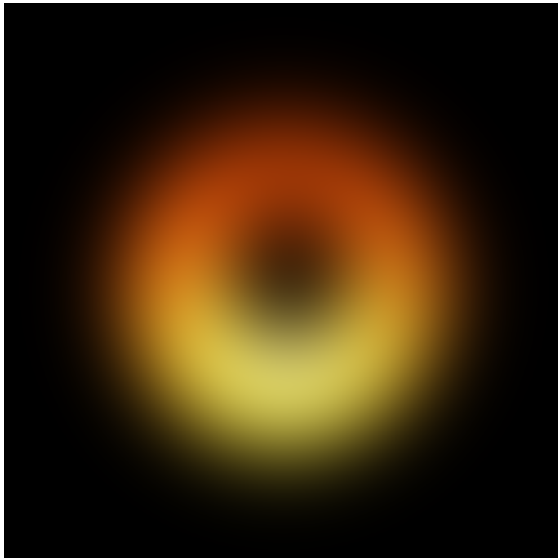


(A) $r_i = 2.91M$

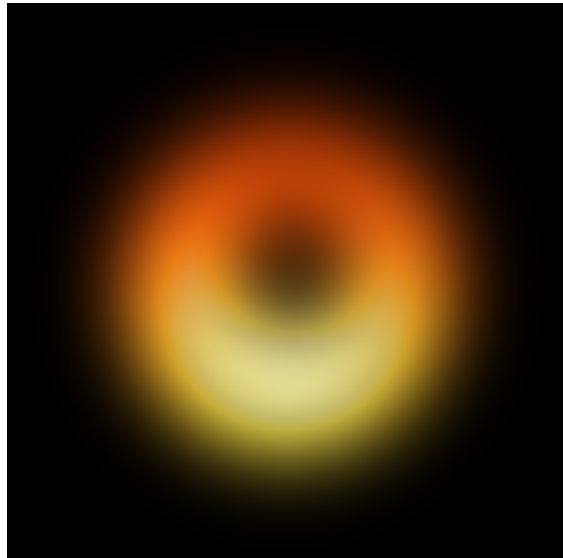


(B) $r_i = 5.82M$

FIGURE 19. Simulations of the black hole M87*.



(A) Blur



(B) Blur and 120% brighter

FIGURE 20. Blurred versions ($\sigma = 50$) of Figure 19a.

APPENDIX A. PROOF THAT THE KNDS METRIC SOLVES THE EINSTEIN-MAXWELL EQUATIONS

The Christoffel symbols of the KNds metric are as follows (their symmetry allows to lighten the notation with bullets):

$$\begin{aligned}
 \Gamma^t_{\mu\nu} &= \frac{1}{\Sigma^2} \begin{pmatrix} 0 & \bullet & \bullet & \bullet \\ \frac{\Delta_r}{\Sigma^2 \chi^2} \left(\frac{1}{2} \Sigma \Delta'_r + r (\Delta_\theta a^2 \sin^2 \theta - \Delta_r) \right) & 0 & 0 & 0 \\ \frac{a^2}{2} \frac{\sin^2 \theta \Sigma \Delta'_\theta + \sin \theta \cos \theta ((a^2 + r^2) \Delta_\theta - \Delta_r)}{\Delta_\theta} & 0 & 0 & 0 \\ \frac{a \sin^2 \theta \left(\frac{1}{2} (a^2 + r^2) \Sigma \Delta'_r - r (\Delta_r (\Sigma + r^2 + a^2) - (a^2 + r^2)^2 \Delta_\theta) \right)}{\Delta_r} & 0 & 0 & 0 \\ \frac{a \sin^2 \theta \left(\frac{1}{2} (a^2 + r^2) \Sigma \Delta'_\theta + a^2 \sin \theta \cos \theta ((a^2 + r^2) \Delta_\theta - \Delta_r) \right)}{\Delta_\theta} & 0 & 0 & 0 \end{pmatrix} \\
 \Gamma^r_{\mu\nu} &= \frac{1}{\Sigma} \begin{pmatrix} \bullet & \bullet & \bullet & \bullet \\ \frac{\Delta_r \left(\frac{1}{2} \Sigma \Delta'_r + r (a^2 \sin^2 \theta \Delta_\theta - \Delta_r) \right)}{\Sigma^2 \chi^2} & 0 & 0 & 0 \\ r - \frac{\Sigma \Delta'_r}{2 \Delta_r} & -a^2 \sin \theta \cos \theta & \bullet & \bullet \\ \bullet & \bullet & -\frac{\Delta_r r}{\Delta_\theta} & \bullet \\ \bullet & \bullet & \bullet & \frac{\Delta_r \sin^2 \theta \left(\frac{1}{2} a^2 \sin^2 \theta \Sigma \Delta'_r - r (a^2 \cos^2 \theta (2 \Delta_\theta (a^2 + r^2) - \Delta_r) + (r^4 - a^4) \Delta_\theta + a^2 \Delta_r) \right)}{\Sigma^2 \chi^2} \end{pmatrix} \\
 \Gamma^\theta_{\mu\nu} &= \frac{1}{\Sigma} \begin{pmatrix} \bullet & \bullet & \bullet & \bullet \\ -\frac{a^2 \sin^2 \theta \Delta_\theta \left(\frac{1}{2} \Sigma \Delta'_\theta + \cot \theta ((a^2 + r^2) \Delta_\theta - \Delta_r) \right)}{\chi^2 \Sigma^2} & 0 & 0 & 0 \\ \bullet & \frac{a^2 \cos \theta \sin \theta \Delta_\theta}{\Delta_r} & r & 0 \\ \bullet & \bullet & -a^2 \cos \theta \sin \theta - \frac{\Sigma \Delta'_\theta}{2 \Delta_\theta} & 0 \\ \bullet & \bullet & \bullet & \frac{\Delta_\theta \sin^2 \theta \left(\frac{1}{2} (a^2 + r^2)^2 \Sigma \Delta'_\theta + \cot \theta ((a^2 + r^2)^3 \Delta_\theta - a^2 \sin^2 \theta \Delta_r (\Sigma + r^2 + a^2)) \right)}{\chi^2 \Sigma^2} \end{pmatrix} \\
 \Gamma^\phi_{\mu\nu} &= \frac{1}{\Sigma^2} \begin{pmatrix} \bullet & \bullet & \bullet & \bullet \\ 0 & \frac{a \left(\frac{1}{2} \Sigma \Delta'_r + r (a^2 \sin^2 \theta \Delta_\theta - \Delta_r) \right)}{\Delta_r} & 0 & 0 \\ \bullet & 0 & 0 & 0 \\ \bullet & \bullet & \bullet & \bullet \\ \bullet & \frac{a \left(\frac{1}{2} \Sigma \Delta'_r + r (a^2 \sin^2 \theta \Delta_\theta - \Delta_r) \right)}{\Delta_r} & 0 & 0 \\ \bullet & 0 & 0 & 0 \\ \bullet & \frac{a^2 \sin^2 \theta \Sigma \Delta'_\theta + \cos \theta ((a^2 + r^2) \Delta_\theta - \Delta_r)}{\Delta_\theta \sin \theta} & 0 & 0 \\ \bullet & \bullet & \bullet & \bullet \\ \bullet & -\frac{\frac{1}{2} a^2 \sin^2 \theta \Sigma \Delta'_r + r (a^2 + r^2) (a^2 \sin^2 \theta \Delta_\theta - \Delta_r)}{\Delta_r} & 0 & 0 \\ \bullet & \frac{\frac{1}{2} \sin \theta ((a^2 + r^2) \Sigma \Delta'_\theta + \cos \theta ((a^2 + r^2)^2 - a^2 \sin^2 \theta \Sigma) - a^2 \sin^2 \theta \Delta_r)}{\Delta_\theta \sin \theta} & 0 & 0 \end{pmatrix}
 \end{aligned}$$

From these we deduce that the only non-zero components of the Ricci tensor are the following:

$$\begin{aligned} R_{tt} &= \frac{1}{\chi^2 \Sigma^3} \left[-\frac{1}{2} a^2 \sin^2 \theta \Sigma \Delta_\theta \Delta_\theta'' + \frac{1}{2} \Sigma \Delta_r \Delta_r'' - a^2 \sin \theta \cos \theta \left(\left(\frac{1}{2} \Sigma + r^2 + a^2 \right) \Delta_\theta + \Delta_r \right) \Delta_\theta' \right. \\ &\quad \left. - r(a^2 \sin^2 \theta \Delta_\theta + \Delta_r) \Delta_r' - a^2 \sin^2 \theta (a^2 - r^2) \Delta_\theta^2 - 2a^2 \cos^2 \theta \Delta_\theta \Delta_r + \Delta_r^2 \right] \\ &= \frac{Q^2 (\Delta_r + a^2 \sin^2 \theta \Delta_\theta)}{\chi^2 \Sigma^3} - \frac{\Lambda (\Delta_r - a^2 \sin^2 \theta \Delta_\theta)}{\chi^2 \Sigma}, \end{aligned}$$

$$\begin{aligned} R_{t\phi} &= R_{\phi t} = \frac{a \sin \theta}{\chi^2 \Sigma^3} \left[\frac{1}{2} \sin \theta (a^2 + r^2) \Sigma \Delta_\theta \Delta_\theta'' - \frac{1}{2} \sin \theta \Sigma \Delta_r \Delta_r'' + \cos \theta \left((a^2 + r^2) \left(\frac{1}{2} \Sigma + r^2 + a^2 \right) \Delta_\theta + a^2 \sin^2 \theta \Delta_r \right) \Delta_\theta' \right. \\ &\quad \left. + \sin \theta (r \Delta_r' (\Delta_r + (a^2 + r^2) \Delta_\theta) + (a^4 - r^4) \Delta_\theta^2 + \Delta_r \Delta_\theta (a^2 \cos^2 \theta - r^2) - \Delta_r^2) \right] \\ &= - \frac{a \sin^2 \theta Q^2 (\Delta_r + (r^2 + a^2) \Delta_\theta)}{\chi^2 \Sigma^3} - \frac{\Lambda a \sin^2 \theta ((r^2 + a^2) \Delta_\theta - \Delta_r)}{\chi^2 \Sigma}, \end{aligned}$$

$$R_{rr} = \frac{1}{\Sigma \Delta_r} \left[-\frac{1}{2} \Sigma \Delta_r'' + a^2 (1 + \cos^2 \theta) \Delta_\theta + a^2 \cos \theta \sin \theta \Delta_\theta' + r \Delta_r' - \Delta_r \right] = -\frac{Q^2}{\Sigma \Delta_r} + \frac{\Lambda \Sigma}{\Delta_r},$$

$$R_{\theta\theta} = \frac{1}{\sin \theta \Sigma \Delta_\theta} \left[-\frac{1}{2} \sin \theta \Sigma \Delta_\theta'' - \cos \theta \left(\frac{1}{2} \Sigma + r^2 + a^2 \right) \Delta_\theta' - \sin \theta (r \Delta_r' + (a^2 - r^2) \Delta_\theta - \Delta_r) \right] = \frac{Q^2}{\Sigma \Delta_\theta} + \frac{\Lambda \Sigma}{\Delta_\theta},$$

$$\begin{aligned} R_{\phi\phi} &= \frac{\sin \theta}{\chi^2 \Sigma^3} \left[-\frac{1}{2} \sin \theta (a^2 + r^2)^2 \Sigma \Delta_\theta \Delta_\theta'' + \frac{1}{2} a^2 \sin^3 \theta \Sigma \Delta_r \Delta_r'' - \cos \theta \Delta_\theta' \left((a^2 + r^2)^2 \left(\frac{1}{2} \Sigma + r^2 + a^2 \right) \Delta_\theta + a^4 \sin^4 \theta \Delta_r \right) \right. \\ &\quad \left. - \sin \theta (r \Delta_r' ((a^2 + r^2)^2 \Delta_\theta + a^2 \sin^2 \theta \Delta_r) + (a^2 - r^2) (a^2 + r^2)^2 \Delta_\theta^2 - \Delta_r \Delta_\theta (a^4 \cos^4 \theta + 2a^2 r^2 + r^4) - a^2 \sin^2 \theta \Delta_r^2) \right] \\ &= \frac{Q^2 \sin^2 \theta (a^2 \sin^2 \theta \Delta_r + (r^2 + a^2)^2 \Delta_\theta)}{\chi^2 \Sigma^3} - \frac{\Lambda \sin^2 \theta (a^2 \Delta_r - (r^2 + a^2)^2 \Delta_\theta)}{\chi^2 \Sigma}. \end{aligned}$$

Therefore, the Ricci tensor can be written as $R_{\mu\nu} = Q^2 R_{\mu\nu}^{\text{ch}} + \Lambda g_{\mu\nu}$, where

$$R_{\mu\nu}^{\text{ch}} := \frac{1}{\chi^2 \Sigma} \begin{pmatrix} \frac{\Delta_r + a^2 \sin^2 \theta \Delta_\theta}{\Sigma^2} & 0 & 0 & -\frac{a \sin^2 \theta (\Delta_r + (r^2 + a^2) \Delta_\theta)}{\Sigma^2} \\ 0 & -\frac{\chi^2}{\Delta_r} & 0 & 0 \\ 0 & 0 & \frac{\chi^2}{\Delta_\theta} & 0 \\ -\frac{a \sin^2 \theta (\Delta_r + (r^2 + a^2) \Delta_\theta)}{\Sigma^2} & 0 & 0 & \frac{\sin^2 \theta (a^2 \sin^2 \theta \Delta_r + (r^2 + a^2)^2 \Delta_\theta)}{\Sigma^2} \end{pmatrix}.$$

As $g^{\mu\nu} R_{\mu\nu}^{\text{ch}} = 0$, the Ricci scalar is $R = g^{\mu\nu} R_{\mu\nu} = 4\Lambda$, the Einstein tensor reads $G_{\mu\nu} = R_{\mu\nu} - \frac{1}{2} R g_{\mu\nu} = Q^2 R_{\mu\nu}^{\text{ch}} - \Lambda g_{\mu\nu}$ and we obtain

$$G_{\mu\nu} + \Lambda g_{\mu\nu} = Q^2 R_{\mu\nu}^{\text{ch}}.$$

Consider now the electromagnetic vector potential

$$A_\mu = \frac{rQ}{\chi\Sigma} (dt - a \sin^2 \theta d\phi).$$

The associated electromagnetic field tensor $F = dA$ has coordinates $F_{\mu\nu} = \nabla_\mu A_\nu - \nabla_\nu A_\mu = \partial_\mu A_\nu - \partial_\nu A_\mu$ and is given by

$$F_{\mu\nu} = \frac{Q}{\chi\Sigma^2} \begin{pmatrix} 0 & r^2 - a^2 \cos^2 \theta & -2ra^2 \cos \theta \sin \theta & 0 \\ a^2 \cos^2 \theta - r^2 & 0 & 0 & a \sin^2 \theta (r^2 - a^2 \cos^2 \theta) \\ 2ra^2 \cos \theta \sin \theta & 0 & 0 & -2ar \cos \theta \sin \theta (r^2 + a^2) \\ 0 & a \sin^2 \theta (a^2 \cos^2 \theta - r^2) & 2ar \cos \theta \sin \theta (r^2 + a^2) & 0 \end{pmatrix}$$

Raising the indices yields the associated contravariant tensor

$$F^{\mu\nu} = g^{\mu\alpha} F_{\alpha\beta} g^{\beta\nu} = \frac{\chi Q}{\Sigma^3} \begin{pmatrix} 0 & (r^2 + a^2)(a^2 \cos^2 \theta - r^2) & 2ra^2 \cos \theta \sin \theta & 0 \\ (r^2 + a^2)(r^2 - a^2 \cos^2 \theta) & 0 & 0 & a(r^2 - a^2 \cos^2 \theta) \\ -2ra^2 \cos \theta \sin \theta & 0 & 0 & -2ra \cot \theta \\ 0 & a(a^2 \cos^2 \theta - r^2) & 2ra \cot \theta & 0 \end{pmatrix}.$$

It is easy to check that for $\nu = t, \phi$, we have $\partial_r(\sqrt{-g}F^{r\nu}) + \partial_\theta(\sqrt{-g}F^{\theta\nu}) = 0$ where $g = \det(g_{\mu\nu}) = -\chi^{-4} \sin^2 \theta \Sigma^2$. Because $\nabla_\mu F^{\mu\nu} = \frac{1}{\sqrt{-g}} \partial_\mu(\sqrt{-g}F^{\mu\nu})$, we obtain that for all ν , we have

$$\nabla_\mu F^{\mu\nu} = 0.$$

Hence, the tensor F is a vacuum solution of the Maxwell equations.

We compute the trace

$$F_{\alpha\beta} F^{\alpha\beta} = 2 \left(\frac{4Q^2 a^2 r^2 \cos^2 \theta}{\Sigma^4} - \frac{Q^2 (r^2 - a^2 \cos^2 \theta)}{\Sigma^4} \right) = 2(B^2 - E^2)$$

and the stress-energy tensor

$$T_{\mu\nu} = \frac{1}{\mu_0} \left(g^{\alpha\beta} F_{\alpha\mu} F_{\beta\nu} - \frac{1}{4} g_{\mu\nu} F_{\alpha\beta} F^{\alpha\beta} \right) = \frac{Q^2}{8\pi\chi^2\Sigma} \begin{pmatrix} \frac{\Delta_r + a^2 \sin^2 \theta \Delta_\theta}{\Sigma^2} & 0 & 0 & -\frac{a \sin^2 \theta (\Delta_r + (r^2 + a^2) \Delta_\theta)}{\Sigma^2} \\ 0 & -\frac{\chi^2}{\Delta_r} & 0 & 0 \\ 0 & 0 & \frac{\chi^2}{\Delta_\theta} & 0 \\ -\frac{a \sin^2 \theta (\Delta_r + (r^2 + a^2) \Delta_\theta)}{\Sigma^2} & 0 & 0 & \frac{\sin^2 \theta (a^2 \sin^2 \theta \Delta_r + (r^2 + a^2)^2 \Delta_\theta)}{\Sigma^2} \end{pmatrix} = \frac{Q^2}{8\pi} R_{\mu\nu}^{\text{ch}} = \frac{G_{\mu\nu} + \Lambda g_{\mu\nu}}{8\pi}$$

and so the EME is indeed satisfied by the KNdS metric and the vector potential A_μ . \square

REFERENCES

- [BBS89] V. Balek, J. Bičák, and Z. Stuchlík. The motion of the charged particles in the field of rotating charged black holes and naked singularities. *Bulletin of the Astronomical Institutes of Czechoslovakia*, 40(2):133–165, 1989.
- [BL67] R. H. Boyer and R. W. Lindquist. Maximal analytic extension of the kerr metric. *Journal of Mathematical Physics*, 8(2):265–281, 1967.
- [BRSS18] N. Bou-Rabee and J. M. Sanz-Serna. Geometric integrators and the hamiltonian monte carlo method. *Acta Numerica*, 27:113–206, 2018.
- [Car68] B. Carter. Global structures of the kerr family of gravitational fields. *Physical Review*, 174(5):1559–1571, 1968.
- [Car95] B. C. Carlson. Numerical computation of real or complex elliptic integrals. *Numerical Algorithms*, 10(1):13–26, 1995.
- [CGL90] R. Coquereaux, A. Grossmann, and B. E. Lautrup. Iterative method for calculation of the weierstrass elliptic function. *IMA Journal of Numerical Analysis*, 10:119–128, 1990.
- [Col20] The Planck Collaboration. Planck 2018 results. vi. cosmological parameters. *Astronomy and Astrophysics*, 641, 2020.
- [DGML09] J. C. Dolence, C. F. Gammie, M. Mościbrodzka, and P. K. Leung. **grmonty**: A monte carlo code for relativistic radiative transport. *The Astrophysical Journal Supplement Series*, 184(2):387–424, 2009.
- [FQ10] K. Feng and M. Qin. *Symplectic geometric algorithms for Hamiltonian systems*. Springer–Zhejiang Publishing, 2010.
- [FW04] S. V. Fuerst and K. Wu. Radiation transfer of emission lines in curved space-time. *Astronomy and Astrophysics*, 424(3):733–746, 2004.
- [GH77] G. W. Gibbons and S. W. Hawking. Cosmological event horizons, thermodynamics, and particle creation. *Physical Review D*, 15(10):2738–2751, 1977.
- [GV12] G. W. Gibbons and M. Vyska. The application of weierstrass elliptic functions to schwarzschild null geodesics. *Classical and Quantum Gravity*, 29(6), 2012.
- [GVW⁺21] E. Gourgoulhon, F. Vincent, M. Wielgus, M. Abramowicz, J.-P. Lasota, T. Paumard, and G. Perrin. Geometric modeling of m87* as a kerr black hole or a non-kerr compact object. *Astronomy & Astrophysics*, 646:A.37, 2021.
- [Hag30] Y. Hagihara. Theory of the relativistic trajectories in a gravitational field of Schwarzschild. *Japanese Journal of Astronomy and Geophysics*, 8:67–176, 1930.
- [Hin80] A. C. Hindmarsh. lsode and lsodi, two new initial value ordinary differential equation solvers. *ACM-Signum newsletter*, 15(4):10–11, 1980.
- [HLW03] E. Hairer, C. Lubich, and G. Wanner. Geometric numerical integration illustrated by the störmer-verlet method. *Acta Numerica*, 12:399–450, 2003.
- [HMS14] S. Heisnam, I. Ablu Meitei, and K. Yugindro Singh. Motion of a test particle in the kerr-newman de/anti de sitter space-time. *International Journal of Astronomy and Astrophysics*, 4:365–373, 2014.
- [HS17] S. Heisnam and K. Yugindro Singh. Geodesics in the kerr–newman anti de sitter spacetimes. *Advances in Astrophysics*, 2(2):95–102, 2017.
- [HV21] S. J. Hoque and A. Virmani. The kerr-de sitter spacetime in bondi coordinates. *Classical and Quantum Gravity*, 38(22), 2021.
- [KK09] N. Kamran and A. Krasinski. Editorial note to: Brandon carter, black hole equilibrium states part i. analytic and geometric properties of the kerr solutions. *General Relativity and Gravitation*, 41:2873–2938, 2009.
- [Kra22] G. V. Kraniotis. Curvature invariants for accelerating kerr-newman black holes in (anti-)de sitter spacetime. *Classical and Quantum Gravity*, 39(14), 2022.
- [LL80] L. D. Landau and E. M. Lifshitz. *The classical theory of fields*, volume 2 of *Course of theoretical Physics*. Butterworth–Heinemann, fourth edition edition, 1980.
- [Pra14] P. Pradhan. Black hole interior mass formula. *European Physical Journal C*, 74(2887), 2014.
- [Pri81] J. E. Pringle. Accretion disks in astrophysics. *Annual Review of Astronomy and Astrophysics*, 19:137–162, 1981.
- [PYYY16] H. Pu, K. Yun, Z. Younsi, and S. Yoon. **Odyssey**: A public gpu-based code for general-relativistic radiative transfer in kerr spacetime. *The Astrophysical Journal*, 820(2):105–116, 2016.
- [Spr95] H. C. Spruit. Accretion Disks. In M. A. Alpar, U. Kiziloglu, and Jan van Paradijs, editors, *The Lives of the Neutron Stars*, volume 450 of *NATO Advanced Study Institute (ASI) Series C*, pages 355–376, 1995.
- [SS73] N. I. Shakura and R. A. Sunyaev. Black holes in binary systems. observational appearance. *Astronomy and Astrophysics*, 24:337–355, 1973.

- [SSC94] J. M. Sanz-Serna and M. P. Calvo. *Numerical Hamiltonian problems*, volume 7 of *Applied Mathematics and mathematical computation*. Chapman & Hall, 1994.
- [VALPO22] J. M. Velásquez-Cadavid, J. A. Arrieta-Villamizar, F. D. Lora-Clavijo, O. M. Pimentel, and J. E. Osorio-Vargas. **OSIRIS**: a new code for ray tracing around compact objects. *European Physical Journal C*, 82(103), 2022.

UNIVERSITÉ DE PICARDIE,
DÉPARTEMENT DE MATHÉMATIQUES ET LAMFA (UMR 7352 DU CNRS),
33 RUE ST LEU,
F-80039 AMIENS CEDEX 1,
FRANCE

Email address: arthur.garnier@u-picardie.fr